Predicting Mangrove Leaf Chemical Content from Hyperspectral Remote Sensing using Advanced Regression Techniques

Christoffer Axelsson

March, 2011

Course Title:	Geo-Information Science and Earth Observation for Environmental Modelling and Management
Level:	Master of Science (MSc)
Course Duration:	September 2009 – March 2011
Consortium partners:	University of Southampton (UK) Lund University (Sweden) University of Warsaw (Poland) University of Twente, Faculty ITC (The Netherlands)

Predicting Mangrove Leaf Chemical Content from Hyperspectral Remote Sensing using Advanced Regression Techniques

by

Christoffer Axelsson

Thesis submitted to the University of Twente, faculty ITC, in partial fulfilment of the requirements for the degree of Master of Science in Geo-information Science and Earth Observation for Environmental Modelling and Management

Thesis Assessment Board

Prof. Dr. Andrew Skidmore (Chair)
Dr. Jadu Dash (External examiner)
Dr. Martin Schlerf (First supervisor)
Prof. Dr. Wouter Verhoef (Second supervisor)

Disclaimer

This document describes work undertaken as part of a programme of study at the University of Twente, Faculty ITC. All views and opinions expressed therein remain the sole responsibility of the author, and do not necessarily represent those of the university.

Abstract

Leaf biochemicals, such as nitrogen, are central to understanding net primary production, photosynthesis and other physiological processes. The variation of these biochemicals in mangroves is poorly understood, and remote sensing may provide a tool for large-scale canopy monitoring. This study has investigated the applicability of airborne hyperspectral remote sensing and advanced regression techniques in estimating the foliar biochemical content. The focus was on two study areas in Indonesia, located in the Berau delta and the Mahakam delta. Leaf samples were collected in these areas during fieldwork in September 2009, and September 2010. The measured foliar biochemical content was then matched with hyperspectral reflectance data of the sample plots to establish predictive models.

Four different regression techniques, ε-SVR, ν-SVR, LS-SVR, and PLSR, were systematically compared. Their performance, as well as their weaknesses and strengths, were evaluated and discussed. In addition, several spectral transformation methods were compared in a similar manner. LS-SVR combined with continuum-removed derivative reflectance (CRDR) yielded the highest prediction results for nitrogen for both the Berau dataset (R^2=0.67, RMSE=0.17, nRMSE=15%) , and the Mahakam dataset (R^2=0.69, RMSE=0.12, nRMSE=11%). For optimal performance of the SVR-based methods, it was necessary to narrow down the number of spectral bands used in the models. The bands of highest relative importance were identified using the regression coefficients of the generated models. The identified wavelength bands could in most cases be linked to previously known absorption features related to nitrogen content.

Predictive models were also established for the foliar content of phosphorus, potassium, calcium, magnesium, and sodium. The performance of these models were either poor, or strongly linked to species composition. While nitrogen can be estimated from its relationship with chlorophyll and proteins, variation in the content of the other biochemicals cannot be tied to optically active compounds in the leaves.

Maps of nitrogen content of the study areas were then derived from the predictive models, and efforts were made to relate the variation in foliar nitrogen to natural and anthropogenic sources of nutrients, including shrimp ponds and the floodwater. Patterns suggest relationships with the nitrogen concentration in the floodwater and with the tidal amplitude.

Acknowledgements

I would like to thank my supervisors Dr. Martin Schlerf and Prof. Dr. Wouter Verhoef for their support, advice, and critical comments on my thesis work.

I am grateful to Anas Fauzi for organising the fieldwork in Indonesia, and for always receiving me in his room when I had questions. The time in the mangroves was a very memorable experience. I want to thank everybody involved, and especially Loise Wandera. My Indonesian weeks would have been much less interesting and enjoyable without her.

Thanks to my GEM colleagues for the good times we have had during the last one and a half years. I am grateful to the consortium members: University of Southampton, Lund University, University of Warsaw, and University of Twente, and all the representatives from these universities that have been involved in organising the GEM program.

Lastly, thanks to Yanti for support, encouragement, and help with graphic design.

Table of contents

List of figures

List of tables

1. Introduction

"You will find something more in woods than in books. Trees and stones will teach you that which you can never learn from masters."

Bernard of Clairvaux (1090 - 1153)

1.1. Background

The content of nitrogen, phosphorus and other nutrients in vegetation foliage can be linked to important ecosystem processes, such as photosynthesis, net primary production, as well as plant health. The variation of these biochemicals in mangroves is poorly understood, and the ability to accurately monitor them would provide important insight into the functions and health status of these ecosystems. The field of hyperspectral remote sensing has developed rapidly in the last decades and can provide the necessary tools for large scale biochemical mapping. This study has explored the possibility to map mangrove foliage content of nitrogen (N), phosphorus (P), potassium (K), calcium (Ca), magnesium (Mg) and sodium (Na) in two study areas in East Kalimantan, Indonesia. The study areas, located in the Mahakam delta and the Berau delta, are very different in terms of anthropogenic disturbances. While the Berau delta is relatively pristine and undisturbed, the Mahakam delta has experienced widespread deforestation and fragmentation of its mangroves due to shrimp pond establishment. The status of the remaining mangroves is uncertain, but they may be influenced by excessive levels of sedimentation and nutrients caused by upstream deforestation and shrimp pond effluents (Sidik, 2009).

1.1.1. Mangroves and nutrient dynamics

Mangrove forests grow in intertidal coastal habitats in the tropics and subtropics. Globally, they are under pressure from the expansion of human activities. Forests are cut down to create new land for agriculture, aquaculture and urban settlements (Giri et al., 2008). Fuelled by scientific evidence supporting their importance, a turnaround in the view of mangroves has been brought about in the last decade. Mangroves act as nursing areas for young fish and other marine life, which are observed to later migrate to coral reefs and other offshore ecosystems (Nagelkerken et al., 2008). They are also known to capture pollutants, and to prevent coastal erosion by consolidating sediments (Alongi, 2008). These functions support adjacent coastal and offshore environments, as well as the people dependant on these

resources (Walters et al., 2008). Furthermore, their high productivity coupled with long-term carbon deposition, in sediments and the oceans, makes them an important carbon sink (Bouillon et al., 2008). This plethora of services, to other ecosystems and human populations, has helped to justify a wider consideration of mangroves. Indeed, several studies have found their value to far outweigh alternative uses (Aburto-Oropeza et al., 2008; Rönnbäck, 1999; Walton et al., 2006).

Figure 1: *Rhizophora spp*. with characteristic stilt roots (left), and a shrimp pond (right). Both in Berau study area.

Better management of mangrove forests requires better knowledge of their physiological processes, and leaf nutrients are central to understanding these processes. Macronutrients, including nitrogen, phosphorus, potassium, calcium and magnesium, are components of bioorganic compounds, such as chlorophyll, proteins and sugars, that all contribute to plant growth (Mooney, 1986). Foliar nitrogen content can be used as an estimator of forest primary production (Smith et al., 2002), and the strong link is attributed to its role in the chlorophyll molecules for light harvesting, and in carbon fixing molecules (Kokaly et al., 2009). Phosphorus is a component of many essential molecules in plants and is vital for energy transfer and cell development (Schachtman et al., 1998). Potassium is needed for the photosynthetic process, stomatal activity, protein synthesis, and enzyme activation (Reef et al., 2010). In saline environments, such as mangrove ecosystems, K is also important for maintaining the osmotic balance (Parida & Jha, 2010). In studies and experiments on mangrove nutrition, most focus has been on nitrogen and phosphorus. Usually, they are limited by low availability of either N, or P, and sometimes both (Krauss et al., 2008; Lovelock et al., 2004). While mangroves are less limited by the availability of potassium, calcium and magnesium due to their ampleness in sea water (Alongi, 2011), also these nutrients can influence mangrove

growth, for instance in the form of species composition (Ukpong, 2000). In general, mangroves are highly sensitive to varying nutrient levels and the effect on plants can be significant. Common physiological changes include raised growth rates with more allocation of biomass in foliage relative to roots (Yates et al., 2002), increased hydraulic conductivity, higher rates of photosynthesis, and lower efficiency in nutrient resorption (Lovelock et al., 2004). Higher nutrient availability also leads to higher foliar concentrations of these biochemicals (Alongi, 2011; Feller et al., 2003; Oxmann et al., 2010), enabling the nutritional status to be detected from the leaves.

Most previous studies on the spatial variability of nutrients have been conducted on Caribbean/South American or Australian mangroves (Boto & Robertson, 1990; Feller et al., 2003; Lovelock et al., 2007). Indonesian mangroves have received less attention, despite the fact that Indonesia accounts for almost 23% of global mangrove area (Giri et al., 2011), and has the highest biodiversity rates worldwide (FAO, 2007). American studies indicate that the nutrient status can vary dramatically, both within and between communities (Feller et al., 2003), but the underlying processes are still not fully understood (Dittmar & Lara, 2001). Commonly, mangroves grow in nutrient poor soils, and many species are well adapted to these conditions. General traits include nutrient-conserving strategies, efficient nutrient cycling, and a high level of plasticity which enables them to withstand poor nutrient conditions while still being able to take advantage of nutrient rich conditions and increase productivity accordingly (Reef et al., 2010). The efficiency with which mangroves can take up and use a specific nutrient can be linked to redox potential, pH, the availability of other limiting nutrients, and the level of salinity (Oxmann et al., 2010; Yates et al., 2002). High salinity can inhibit the uptake of nitrogen and potassium, leading to lower growth rates (Kao et al., 2001; Naidoo, 1987).

The availability of nutrients can be linked to various biotic and abiotic factors, including the microbial activity in the soil, litter production and decomposition, and the degree of tidal inundation (Reef et al., 2010). Mangroves exchange nutrients with the floodwater, and the degree of nutrient exchange can be linked to the concentration of nutrients in the floodwater and the tidal amplitude (Adame & Lovelock, 2011; Childers et al., 2002). In cases of higher nutrient concentrations in the floodwater, mangroves take up dissolved inorganic nutrients from the water, and export them in organic form as litter.

In many areas, anthropogenic sources of nutrients play a major role. Shrimp pond effluents is one such source, which has been shown to cause elevated nitrogen levels in surrounding mangroves (Costanzo et al., 2004). The contaminating effect of

shrimp ponds depends on if they are managed extensively or intensively. In extensive aquaculture, no extra nutrients are added and the effluent may have lower nutrient concentrations than the water flowing into the ponds. In contrast, intensive aquaculture is based on adding nutrients to feed the shrimps, and large amounts of these nutrients can leak to the surrounding environment (Martin, 2011). Although eutrophication may be harmful to mangroves under specific conditions in fertilisation experiments (Lovelock et al., 2009), most evidence underline their capacity to withstand and take advantage of high nutrient levels. Indeed, their high productivity and ability to absorb pollutants make them suitable to use for removing nutrients and heavy metals from contaminated waters (Tam et al., 2009; Zhang et al., 2010). There is, however, high interspecies variability in their ability to cope with anthropogenic disturbances. Signs of plant stress in mangrove ecosystems may even be masked by the transition from vulnerable to more resilient species (sensu Dahdouh-Guebas et al., 2005).

1.1.2. Remote sensing of leaf biochemistry

The reflectance spectra from vegetation carry information on its biochemical constituents. Leaf pigments such as chlorophyll are active in the wavelength region of highest solar input between 0.4 and 0.70 µm, while non-pigment constituents such as proteins, lignin, cellulose and water can be detected in the infrared region from 0.7 to 2.5 µm (Kokaly et al., 2009). Detection of these constituents is rendered possible through scattering and absorption effects caused by vibrations in the chemical bonds within the compounds. Absorption features of biochemicals in the near and short-wave infrared are the result of overtones and harmonics of stronger principal absorption features in longer wavelengths (Curran, 1989). The works of Curran (1989) and Kokaly & Clark (1999) demonstrated the possibility to estimate the biochemical content in dried leaves using spectroscopy and stepwise regression. Many studies have applied similar techniques on fresh leaves (Curran et al., 1992), and on forest canopies using airborne or satellite-borne reflectance data (Martin et al., 2008). The ultimate, most cost-efficient and consistent way would be to monitor foliar biochemicals using space-based sensors. However, each step brings obstacles that lower the accuracy of estimates. When extending analysis from dried to fresh leaves, the leaf water constitutes the main barrier by obscuring absorption features of other biochemicals (N. M. Knox et al., 2010; Kokaly et al., 1999). When analysing whole canopies, the additional effect of vegetation structure, illumination effects, atmospheric scattering and absorption, the signal-to-noise ratio, and the reflectance from undergrowth, soil, roots and branches must be taken into consideration (Asner & Martin, 2008; Majeke et al., 2008).

Table 1: Examples of studies on remote sensing of forest biochemicals.

Chem.	R^2	nRMSE	Scale	Vegetation	Reference
N	0.94	0.24%	Leaf (dried)	Slash pine	(Curran et al., 2001)
N	0.86	-	Leaf (fresh)	Woody plants	(Ferwerda & Skidmore, 2007)
N	0.53	21%	Canopy	Temperate forest	(Huber et al., 2008)
N	0.57	5%	Canopy	Norway spruce	(Schlerf et al., 2010)
N	0.65	26%	Canopy	Tropical forest	(Asner et al., 2008)
N	0.83	13%	Canopy	Range of forest ecosystems	(Martin et al., 2008)
P	0.74	7%	Leaf (dried)	Slash pine	(Curran et al., 2001)
P	0.51	-	Leaf (fresh)	Woody plants	(Ferwerda et al., 2007)
P	0.36	42%	Canopy	Tropical forest	(Asner et al., 2008)
K	0.68	-	Leaf (fresh)	Woody plants	(Ferwerda et al., 2007)
Ca	0.62	-	Leaf (fresh)	Woody plants	(Ferwerda et al., 2007)
Mg	0.49	-	Leaf (fresh)	Woody plants	(Ferwerda et al., 2007)
Na	0.60	-	Leaf (fresh)	Woody plants	(Ferwerda et al., 2007)

Few studies have attempted to estimate P, K, Mg, Ca and Na, and high prediction performance for these biochemicals at the canopy level is yet to be achieved. They are optically inactive, and their content is difficult to trace in the canopy spectra. Nitrogen, on the other hand, has been in focus for many remote sensing efforts, and can be estimated through its relationship with chlorophyll and proteins (Kokaly et al., 2009; Wright et al., 2004). The relationship between nitrogen and chlorophyll is most pronounced in N limited environments and can be much weaker in ecosystems not limited by the availability of N (Kokaly et al., 2009). Usually, studies take place in less complex ecosystems with a small number of tree species. Experiences from mixed forests show that the composition of species together with leaf area index (LAI) are the predominant drivers of variation in reflectance (Asner, 2008). For vegetation covers of less than 70-80%, gap fraction is the most influential factor on the spectral signature (Asner, 2008; Baret et al., 1995), and a dense forest canopy therefore represents the ideal setting for estimation of leaf chemicals (Asner, 1998). Vegetation factors that influence reflectance include the leaf angle distribution, leaf thickness, and multiple scattering and shadow effects caused by the canopy structure (Barton & North, 2001; Kupiec & Curran, 1995). Varying LAI and covariance between the biochemical content and the vegetation structure of different species, therefore constitutes a major problem in foliar biochemical estimation and it is important to find ways to counteract these factors.

1.1.3. Modelling the nutrient content

There are two major approaches to modelling the biochemical content in vegetation: physical and empirical modelling. Physicals models are based on calculating the interaction of electromagnetic radiation with vegetation, and the resulting canopy reflection model can simulate the spectral signal detected by the sensor using information on vegetation properties. For retrieval of vegetation properties from the spectral signal, the model is inverted. Although physical models are claimed to be relatively robust (Jacquemoud et al., 2009), and more portable than empirical models (Schlerf & Atzberger, 2006), they were not deemed suitable in this study. While existing physical models, such as the Soil-Leaf-Canopy model (Verhoef & Bach, 2007), can be used to model chlorophyll content in forest canopies, they are not designed to retrieve the content of nitrogen or other nutrients. Nitrogen could then only be estimated from its relationship with chlorophyll, which may or may not be strong.

In contrast, the empirical approach can be used to model any foliar biochemical since it uses statistical regression to establish a relationship between the chemical content and the reflectance signal. Some regression methods, such as partial least squares regression (PLSR), can be applied on the full reflectance spectra, and thus make use of all available information. This enables previously unknown relationships to be used, and then possibly identified during interpretation of the model. Later, found relationships may be physically explained and incorporated into physical models. While most studies on remote sensing of biochemicals rely on empirical models (Huang et al., 2004; Martin et al., 2008; Mutanga et al., 2004; Schlerf et al., 2010), they have some known disadvantages. The established models are generally site and time specific and cannot readily be applied on other kinds of vegetation or under different conditions (Grossman et al., 1996). For instance, in an attempt to map nitrogen on sites covering a wide range of ecosystems, Martin et al. (2008) found that the accuracy of estimations dropped more or less sharply as sites were eliminated from the calibration set and predicted using data from the other sites.

PLSR has been used extensively in biochemical modelling (Asner, 2008; Atzberger et al., 2010; Darvishzadeh et al., 2008) and is particularly suited to handle cases with noisy and collinear variables, or when the number of independent variables exceeds the number of observations (Wold et al., 2001). One comparatively new regression approach that has shown great promise in many applications is support vector regression (SVR). It has, for instance, outperformed PLSR in applications for industrial chemometrics (Thissen, Pepers, et al., 2004), and for predicting protein

fractions in alfalfa using spectroscopy (Nie et al., 2008). Previous applications of SVR in the field of hyperspectral remote sensing are, however, few in number and this study has further explored its performance as well as its interpretability.

1.2. Research problem

Remote sensing has previously been employed to map the extent and species composition of mangroves, and to estimate their biomass and leaf area (Heumann, 2011). To my knowledge, no previous study has estimated the biochemical content of mangroves from remote sensing imagery. Research is needed; both in terms of understanding the variation of foliar chemicals, and for finding which methods are most useful for analysing and mapping it. The problems addressed by this study are:

- How to develop predictive models for retrieving the foliar biochemical content of mangroves.
- To understand the spatial variation of foliar biochemicals in mangroves with respect to anthropogenic and natural sources of nutrients.

1.3. Research objectives

a) Analyse the possibility to retrieve mangrove foliar nutrient concentrations using airborne HyMap images.

b) Explain the models in terms of significant bands and their relation to known biophysical reflection properties of leaves.

c) Evaluate the applicability of support vector regression and partial least squares regression in modelling the biochemical content.

d) Find ways to counteract the influence of varying LAI, and covariance with genera in the generated models and biochemical maps.

e) Analyse the spatial variability of estimated biochemical levels.

1.4. Research questions

a) To which degree can foliar N, P, K, Ca, Mg and Na concentrations be estimated using airborne HyMap images and regression techniques?

b) Which regression technique shows the highest explained variability (R^2) and lowest root-mean-squared error (RMSE)?

c) Can the models be explained? That is, which bands are most important and can these bands be related to known biochemical absorption features?

2. Materials and methods

"Method is much, technique is much, but inspiration is even more."
Benjamin Cardozo (1870 - 1938)

2.1. Study areas

This thesis has focused on two areas located in the Mahakam delta and the Berau delta, East Kalimantan, Indonesia. The two areas are very different in terms of human influence. While the Berau delta is still relatively pristine, most of the Mahakam delta mangroves have been cut down.

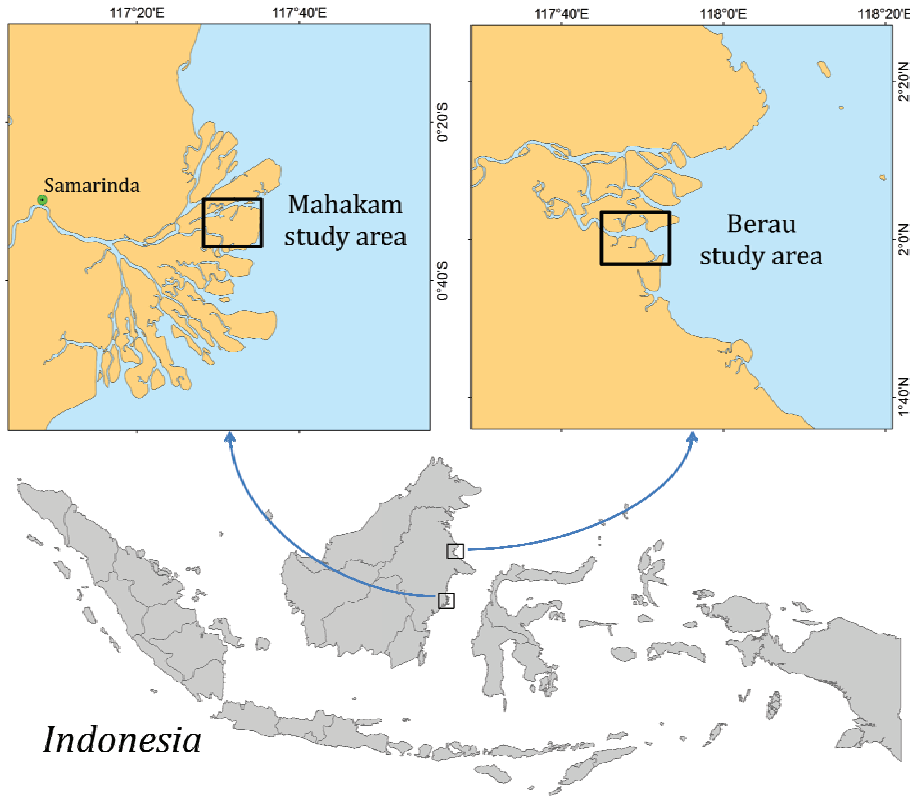

Figure 2: Location of study areas. (Data source: Bakosurtanal, Indonesia, 2000)

2.1.1. Mahakam delta

The Mahakam delta lies east of the provincial capital, Samarinda. The Mahakam River is the largest in Eastern Kalimantan, stretching 770 km, and bringing large amounts of sediments to the fan-shaped delta. Originally, the delta harboured one of the most extensive communities of *Nypa fruticans* in the world. However, most of these and other mangroves were cut down, mainly during the 1990's and early 2000's. It is estimated that about 70% of the deltaic mangroves have disappeared, primarily as a consequence of shrimp pond establishment (Sidik, 2009). Shrimp ponds in the Mahakam delta has traditionally been extensively managed, but intensive farming has been promoted (Powell & Osbeck, 2010). At the time, it is not known to which degree they are intensively managed or to which degree they pollute the water of the delta. One sign of degraded water quality is a collapse in shrimp production (Martin, 2011), and production rates in the Mahakam delta have been in decline for a number of years (Powell et al., 2010; Sidik, 2009). This is probably a result of both increased pollution and the destruction of mangroves. At the present time, Indonesian authorities and local stakeholders are increasingly recognising the economic and environmental benefits of healthy mangrove communities, and some efforts have been put into replanting projects (Powell et al., 2010).

The area where the study took place is situated in the north-eastern part of the delta (lat. 0°29′42″S - 0°35′45″S, long. 117°27′59″E - 117°35′3″E). Remaining mangroves are composed of *Rhizophora spp.*, mono-specific *Nypa fruticans* stands, *Avicennia spp.*, and some sparse *Sonneratia spp.* and *Bruguiera spp.* stands.

2.1.2. Berau delta

The much less disturbed Berau delta is situated 280 km to the north of the Mahakam study area. Off-shore from the delta lies the Derawan archipelago, a biodiversity hotspot for corals and reef fish. Although there are some shrimp pond developments in the delta, it is on a far smaller scale than in Mahakam. The study area (lat. 1°57′2″N - 2°4′31″N, long. 117°44′45″E - 117°54′17″E) is mainly dominated by *Rhizophora spp.* with some *Nypa fruticans* and *Bruguiera spp.* communities. *Avicennia spp.* is common along coastal fringes with saltier water and high inundation levels. Some sparse *Sonneratia spp.* and *Xylocarpus spp.* stands are also present in the area.

2.2. Field data

Fieldwork in Mahakam was conducted in September 2009, and in Berau during September-October 2010. The same sampling strategy was followed during the two campaigns. Samples were collected along transects perpendicular to the shoreline. The best available data on the area was used when planning transect locations. In 2010 it was possible to use the hyperspectral images for this purpose. The aim was to capture the variation in mangrove forest types and growing conditions over the study areas, reflecting the variation in leaf biochemicals. More variation in the chemical content of the samples caters for more robust models. A maximum length of 400 meters from boat landings was estimated to be sufficient for capturing the foliar biochemical variation along transects. Each transect had 5-7 sample points, separated by a distance of approximately 50 meters. A shorter distance between sample points would have made the sampling process slower. Although transects were planned beforehand, local conditions and features not known beforehand did influence the sampling process. Planned transects sometimes changed due to the accessibility of the terrain, or the composition of species in the forest. The coming and going of the tide also create a time-window that restricts arriving and leaving certain locations by boat. The dense forest, often with mud and thick root systems underneath, further constrains accessibility and thereby the number of samples possible to collect in a day. Heterogeneous areas with mixed species were, as far as possible, avoided due to the risk of matching leaf samples with image pixels of the wrong species. Maps of the collected samples can be found in appendix 1. It is acknowledged that the time gap of one year between the recording of the images and the Berau field campaign may cause errors. It is, however, more important that the fieldwork, in both campaigns, was conducted during the same season as when the images were recorded. Previous studies (e.g. Lin et al., 2010) have shown that foliar nutrient content of mangroves can change seasonally.

At each sample point, a representative tree of the dominating genera was selected and then climbed by a local guide. A couple of branches from the upper part of the canopy were cut down and 10 mature non-damaged leaves were collected from these branches. The biochemical content of mangrove leaves change with leaf age and especially during senescence. Usually, foliar nitrogen and phosphorus are resorbed during senescence in order to conserve these nutrients, while Na is accumulated in order to get rid of excess sodium through abscission (Medina et al., 2010; Zhou et al., 2010). More stable measurements should be obtained by only analysing mature non-senescent leaves. The leaves were stored in envelopes before being shipped to the laboratory for chemical analysis. At each sample plot, the position was registered using a GPS receiver with an estimated positional accuracy of 5-10 meters.

2.2.1. Chemical analysis of leaf samples

After fieldwork, the collected leaf samples were delivered to the Mulawarman University in Samarinda, Indonesia, for analysis of the chemical content. Leaves were first dried to a constant weight at 70° C and ground using a Wiley mill. Nitrogen was measured using the Kjeldahl method. Phosphorus content was measured with a BioMate UV-Visible spectrophotometer. The concentrations of K, Ca, Mg and Na were determined with a BioMate atomic absorption spectrometer (AAS). The content of all biochemicals were measured as weight percent of dried matter (%dm).

2.2.2. Sample statistics

Altogether, 25 transects with a total of 138 points were sampled in the study areas. Unfortunately, some of these samples could not be used in the final analysis. Some of the samples in the 2009 campaign were covered by clouds or cloud shadows on the airborne images and had to be discarded. A combination of low positional accuracy and heterogeneous forest at some of the sample plots led to further discards, due to risk of pixel/plot misregistration. In total, 47 samples in Mahakam and 74 in Berau were used in the final prediction models.

Table 2: Sample summary.

Genera	Berau	Mahakam
Avicennia	5	3
Bruguiera	19	1
Nypa	8	16
Rhizophora	38	21
Sonneratia	0	6
Xylocarpus	4	0
total used	74	47

2.3. Hyperspectral imaging

Airborne hyperspectral images were taken with a HyMap sensor (Cocks et al., 1998), which detects radiance in 126 spectral bands with coverage between 0.45 µm and 2.49 µm. The Mahakam images were recorded on 16 October 2009, and the Berau images on 18 October 2009. Due to unstable weather conditions at the time of recording, parts of the images were covered by clouds and cloud shadows.

The images were processed by HyVista, Sydney, Australia. They were converted to top-of-canopy reflectance with the software Hycorr, using a model for atmospheric correction that is similar to MODTRAN. Empirical line calibration was used for reducing spikes around bands affected by water vapour. Geocoding was performed with a parametric procedure and assessment of the geocoding accuracy was based on

measurements of GCP's in the field resulting in an average positional error of 6-9 meters. The spatial resolution of the images is 3.1 meters.

It was found that the reflectance spectra for the Berau images contain more noise than the Mahakam images, which may be attributed to hazier weather conditions at the Berau site. The noise pattern was in the form of horizontal stripes, coinciding with the flight lines of the aircraft. The Berau spectra also had a couple of artefacts, unexpected peaks, in bands at 0.956 µm and 1.12 µm. These and bands above 2.43 µm, which contained high levels of noise, were excluded from the analysis.

When extracting the reflectance values, the pixel spectra were visually checked in order to select pixels with pure vegetation characteristics. Pixels with lower leaf area and higher degree of mud, roots or water were avoided. Though the aim was to use the four pixels closest to the sampling position (Martin & Aber, 1997), a scarcity of pure canopy pixels lead to 2-3 pixels being selected in some cases. The spectra were subsequently averaged to produce the mean spectra for each sample location.

It is well known that appropriate spectral transformation techniques can remove noise and enhance absorption features of biochemicals, thereby improving the accuracy of the regression models (Majeke et al., 2008). Apart from using the untransformed reflectance, four spectral transformation methods were applied and compared in the analysis: MNF-processing, continuum removal, Savitzky-Golay first derivative, and continuum-removed derivative reflectance (CRDR). Continuum-removal, reflectance derivatives, and CRDR have all been used successfully in previous studies using hyperspectral remote sensing (Ferwerda et al., 2007; Huang et al., 2004; Mutanga et al., 2004). The untransformed and MNF-processed spectra were mainly included for comparative reasons.

2.3.1. Minimum noise fraction (MNF)

The minimum noise fraction (MNF) transform, as implemented in ENVI 4.7 (ITT Visual Information Solutions, 2009), was used to remove noise from the images (Green et al., 1988). First, a forward MNF transform was applied, in which data are orthogonalised into a new feature space, based on the estimated noise content. The first MNF transformed bands, with higher eigenvalues, are considered to contain the useful information, while later bands contain most of the noise. A selection of the first bands is then inverted back into the original feature space, producing noise-reduced reflectance data. For the Mahakam image, the first 25 bands were used in the inversion process, while only 11 bands were used for Berau. By being more selective in the choice of bands for Berau, and specifically avoid bands with clear

striping, it was possible to suppress the flight line patterns that lowered the quality of those images. The Berau data was thereby changed to a greater degree in this process than the Mahakam data.

2.3.2. Continuum removal

Continuum removal (CR) is often applied in hyperspectral analysis in order to reduce background effects and enhance absorption features in the spectra (Kokaly et al., 1999). The continuum is a line fitted on top of the spectra, connecting local spectral maxima (figure 3). It is an estimation of general features of the spectra, apart from the biochemical absorption features of interest. The continuum is removed by dividing the original spectral values by the corresponding values of the continuum line. The processing was made in ENVI 4.7 (ITT Visual Information Solutions, 2009), and the MNF-processed spectra were used as input because continuum removal is sensitive to noise in the data. Usually, spectra are subdivided before applying continuum removal on specific absorption features, but the method has also shown great efficiency when applied on the full spectrum (Huang et al., 2004). Here, the spectra were divided into two parts (0.45-1.45 µm, and 1.45-2.43 µm), with the aim of better isolating biochemical absorption features in the latter part.

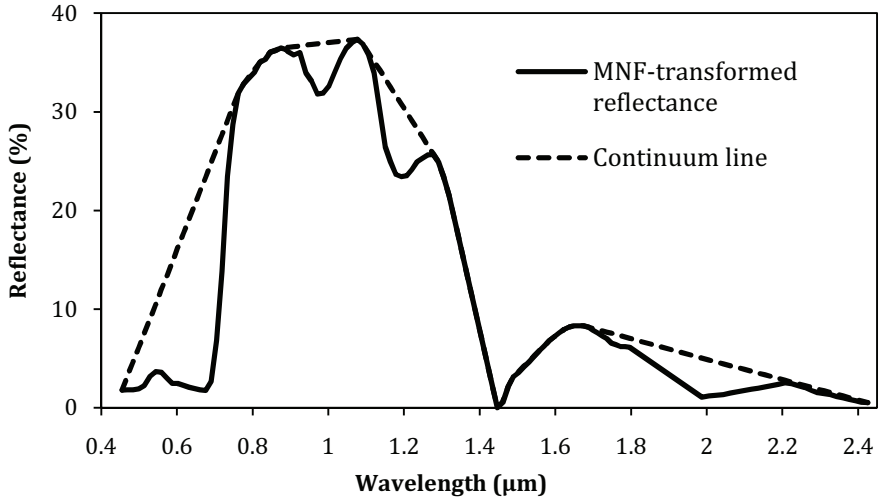

Figure 3: Reflectance spectrum and its continuum line. The continuum was calculated separately for two parts of the spectra (0.45-1.45 µm, and 1.45-2.43 µm).

2.3.3. Savitzky-Golay first derivative

First derivatives were calculated with the Savitzky-Golay smoothing method (Savitzky & Golay, 1964). Because derivatives are highly sensitive to noise in the data, the spectra were smoothed using a five-band moving window (Tsai & Philpot, 1998). A third order polynomial was fitted to the spectral data in the window using a least-square fitting procedure, and the parameters of the polynomial were used to calculate derivatives. The first derivative shows the slope of the reflectance curve, and is often more strongly related to absorption features than the original spectrum. The method was applied on the untransformed reflectance spectra, as well as the continuum-removed bands to produce continuum-removed derivative reflectance (CRDR) (Mutanga et al., 2004).

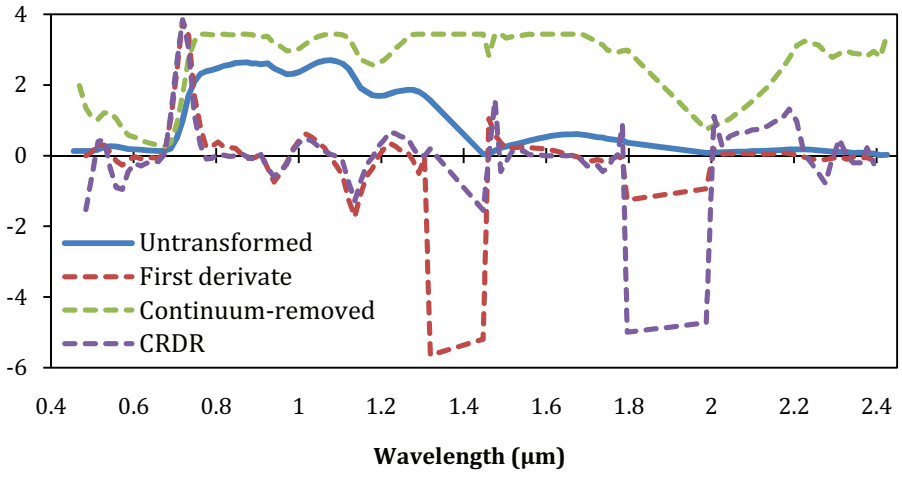

Figure 4: Examples of transformed mangrove reflectance spectra. For comparative reasons, each spectrum was normalised through division by its standard deviation.

2.4. Regression analysis

A characteristic of hyperspectral data is that wavelengths are often correlated, leading to problems with multicollinearity in regression analysis. Also, the number of bands used often exceeds the number of measurements, which can lead to overfitting on the calibration data (Wold et al., 2001). Traditional regression methods, such as stepwise multiple linear regression, are often unable to deal with these problems (Curran, 1989). Although these problems could be overcome by first singling out the spectral bands of interest, this study aimed to start by making use of the full spectra. While absorption features associated with nitrogen have been identified (Curran, 1989), less is known of which bands are important for identifying

the spectral footprint of other foliar nutrients such as phosphorus and magnesium. By initially using the full spectra and then analyse the regression coefficients, it is possible to find out which bands are most informative in each case. These bands are then used to generate the final model.

This study utilised three variants of support vector regression (SVR) and partial least squares regression (PLSR). PLSR has been used frequently in remote sensing studies of vegetation, and has been shown to outperform the more conventional stepwise multiple linear regression (Atzberger et al., 2010; Darvishzadeh et al., 2008). Here, PLSR serves as a proven reference to the comparatively more novel support vector approaches, both in terms of model performance and model interpretation. The other three methods are based on the support vector machine (SVM), developed by Vapnik and colleagues in the early 1990's. SVM is a machine learning technique sprung from the field of statistical learning theory. Since its development it has been successfully used in many fields, including applications for time-series prediction (Cao & Tay, 2004), pattern recognition such as face detection (Osuna et al., 2002), and image classification (Chapelle et al., 2002). Initially, it was developed to solve classification problems but was later extended to also handle regression (Vapnik, 1995). Support vector regression (SVR) uses the principle of structural risk minimisation to simultaneously optimise performance and generalisation, and is often able to find non-linear and unique solutions (Thissen, Üstün, et al., 2004). There are a few different variants of SVR that utilises different optimisation algorithms, and the three most commonly used are perhaps ε-SVR, ν-SVR and LS-SVR. This study has experimented with these three, in order to compare them and find the most appropriate in the present case.

Validation of the results was carried out using standard leave-one-out crossvalidation (Efron & Gong, 1983). One model for each sample was created and the prediction for that sample was calculated using all other samples as calibration set. The process was then repeated for all combinations of spectral transformation and regression method for all foliar biochemicals. Model performance was quantified using precision, by means of the coefficient of determination (R^2), and accuracy, in the form of cross-validated root-mean-squared error. Also the normalised root-mean-squared error (nRMSE or relative error) was calculated by dividing the RMSE with the mean of the sample set.

Prior to the calibration phase, regression parameters were tuned. This is an important step in any empirical regression, and serves to find a suitable level of complexity for the model (Wold et al., 2001). An overly complex model leads to overfitting on the calibration data, and will be less efficient at predicting other samples. All regression

tools had built-in cross-validation functions that were employed in the process, and parameter settings were optimised through minimisation of RMSE. The tuning process is crucial for model performance, and cross-validation methods (both k-fold and leave-one-out) are considered reliable approaches (Chalimourda et al., 2004; Darvishzadeh et al., 2008; Hernández et al., 2009). The complete analysis was carried out in MATLAB v.R2010a (The MathWorks, 2010).

2.4.1. Partial least squares regression

Partial least squares regression (PLSR) combines concepts from multiple linear regression and principal component analysis. It uses component projection to reduce the full spectrum to a smaller number of non-correlated components (also called *latent variables*) that contain the most useful information (Rosipal and Krämer 2006). To a large extent, noise and collinearity in the original spectra is eliminated in the condensed components. The aim was to predict foliar chemical content (Y) from the hyperspectral reflectance data (X). Both the X and Y variables are decomposed as a product of a set of orthogonal components and a set of loadings. As explained by Wold et al. (2001), the PLSR algorithm finds a smaller number of orthogonal variables, X-scores, which both model the original X, and are good predictors of Y. The X-scores (T) are linear combinations of the X-variables and the weights W:

$$\begin{aligned} T &= XW \\ X &= TP' + E \\ Y &= TC' + F \end{aligned} \qquad (1)$$

The original X-matrix is then decomposed into X-scores (T) and X-loadings (P), with minimisation of the residuals in E. The same X-scores can also predict Y through multiplication with the weights (C), where the y-residuals (F) denote the prediction error. The latent variables in the score matrix (T) are designed to explain as much as possible of the covariance between X and Y (Abdi, 2010). The above equations can be combined into:

$$Y = XW * C' + F = XB + F \qquad (2)$$

where B contains the regression coefficients, which determine a linear relationship between X and Y. The regression coefficients thereby also carry information on the influence of each X-variable on the model. The absolute values of the regression coefficients are proportional to the relative importance of their corresponding X-variables for predicting Y, and when plotted alongside the original spectra they enable interpretation of the PLSR-model.

The performance of a model depends on the number of latent variables set by the user. Typically, the performance first increases with more latent variables, and after the optimal number is reached it decreases due to overfitting (Abdi, 2010). Here, the optimal number was determined through five-fold crossvalidation on the calibration set and selecting the setting that minimises RMSE. The plsregress tool in MATLAB v.R2010a (The MathWorks, 2010) was used for regression modelling, including the parameter optimisation.

2.4.2. Epsilon (ε) support vector regression

Epsilon (ε) SVR is the original SVR method developed in the mid 1990's. It was developed to solve the regression problem defined as follows: $\{x_n, y_n\}_{i=1}^{N}$ is a set of calibration data, where $x_i \in R^n$ is the ith data point in input space, and $y_i \in R$ is the corresponding output. The input data are transformed into a high-dimensional feature space using a non-linear function. The aim of ε-SVR is then to approximate a linear function in the high-dimensional feature space of the form:

$$f(x, w) = \langle w * \varphi(x) \rangle + b \qquad (3)$$

where $\langle w * \varphi(x) \rangle$ is the dot product between w and $\varphi(x)$, w is a vector in the feature space, and b is a constant (Haigang et al., 2003; Smola & Schölkopf, 2004). Instead of only trying to minimise the training error (empirical risk), it also aims to minimise the complexity of the model (structural risk). The ability of SVR to control the complexity and thereby produce models with high generalisation performance and less risk of overfitting is one of its main advantages. Minimisation of the training error is handled by Vapnik's ε-insensitive loss function, by which errors are not penalised as long as they are smaller than ε. A loss-free tube with radius ε is thus formed around the data points. Points that fall outside of the tube are penalised according to the deviation of their value from the ε-tube (figure 5).

As explained in Smola and Schölkopf (2004), it can be formulated as a convex optimisation problem with the use of slack variables (ξ_i, ξ_i^*) to help solve the minimisation problem:

$$min \frac{1}{2}\|w\|^2 + C * \frac{1}{n}\sum_{i=1}^{n}(\xi_i + \xi_i^*) \qquad (4)$$

Subject to the constraints:
$$\begin{cases} y_i - \langle w * \varphi(x) \rangle - b \leq \varepsilon + \xi_i^* \\ \langle w * \varphi(x) \rangle + b - y_i \leq \varepsilon + \xi_i \\ \xi_i, \xi_i^* \geq 0, \ i = 1, \ldots, n \end{cases}$$

Here, $\|w\|^2$ characterises model complexity and the second part of the formula takes the training error into account. The regularisation constant C determines the trade-off between model flatness and the degree to which errors larger than ε are penalised. The solution of the described optimisation problem can be obtained by introducing Lagrange multipliers. The regression function then gets the following form:

$$f(x) = \sum_{i=1}^{n} (\alpha_i - \alpha_i^*) K(x_i, x) + b \qquad (5)$$

where $K(x_i, x)$ is a kernel function. The actual support vectors are calibration data on or outside the ε-tube border, and the Lagrange multipliers (α_i, α_i^*) associated with these vectors are called *support values* (Shmilovici, 2005). Calibration data inside the tube are thus not part of the regression model, meaning that a larger set ε reduces the number of support vectors. Both C and ε have a large impact on the performance of ε-SVR and have to be appropriately set before training the model. In this study, they were tuned through a grid search of parameter settings where each setting was evaluated using five-fold cross-validation on the calibration data.

It is the kernel function that transforms the input data into a high-dimension feature space, and thereby enables SVR to map a non-linear relationship using a linear function. There are several different options for which kernel function to use. The most widely recommended (e.g. by Scholkopf et al., 1997), and the one employed in this study, is the Gaussian Radial Basis Function (RBF) with the formula:

$$K(x_i, x) = exp\left(-\frac{\|x - x_i\|^2}{2\sigma^2}\right) \qquad (6)$$

where σ defines the kernel width. Other types, linear and polynomial kernels, were briefly tested, but the RBF kernel was found to be the most reliable in this case. The matlab tools provided in the libSVM software library v3.0 (Chang & Lin, 2001) were used for all ε-SVR, as well as ν-SVR, calculations. Following recommendations in the software manual, all spectral data were normalised to $0 \leq x \leq 1$ before applying the methods.

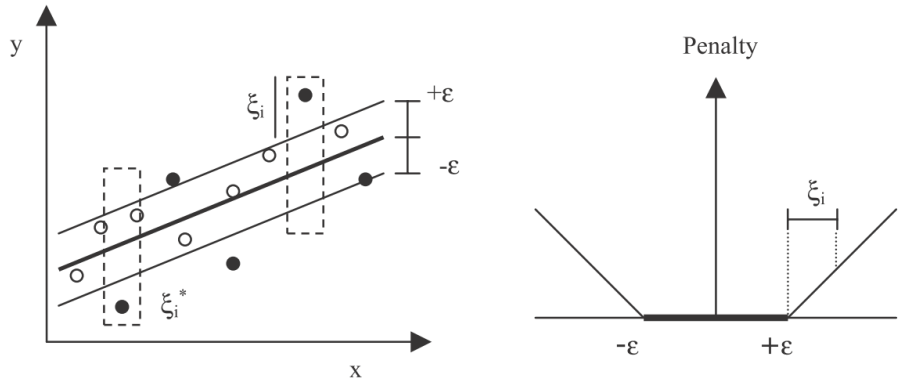

Figure 5: The ε-svr approach, where data points located outside the ε-tube (the support vectors) are penalised according to the deviation ξi. The slopes in the loss-function (right figure) are determined by the C parameter. Figure from Thissen, Pepers et al. (2004).

2.4.3. Nu (ν) support vector regression

Given the difficulty in finding suitable values for the tube-width ε, Schölkopf et al. (2000) proposed a modification of the algorithm that automatically minimises ε depending on the properties of the data. With this method, called ν-SVR, a new parameter (ν) is introduced that trades off the size of ε against model complexity and slack variables. The optimisation equation then gets the form:

$$min\frac{1}{2}\|w\|^2 + C * \left(\nu\varepsilon + \frac{1}{n}\sum_{i=1}^{n}(\xi_i + \xi_i^*)\right) \qquad (7)$$

Subject to the constraints: $\begin{cases} y_i - \langle w * \varphi(x)\rangle - b \leq \varepsilon + \xi_i^* \\ \langle w * \varphi(x)\rangle + b - y_i \leq \varepsilon + \xi_i \\ \varepsilon, \xi_i, \xi_i^* \geq 0,\ i = 1, \ldots, n \end{cases}$

Instead of choosing C and ε a priori, the user will need to specify C and ν, where ν in effect determines a fraction of the data points to be used as support vectors. Again, a grid search and five-fold cross-validation was employed for finding suitable parameter values.

2.4.4. Least squares support vector regression

Least squares (LS) SVR is an alternative variant of SVR proposed by Suykens, Van Gestel and De Brabanter (2002). It simplifies the optimisation problem by replacing the quadratic programming equation (4) with a set of linear equations, making it computationally faster (Shmilovici, 2005). The insensitive loss function is replaced

by a squared loss function. LS-SVR requires the setting of two parameters, the kernel parameter (σ^2) and the regularisation factor (γ). In practise, this step was greatly facilitated by a new optimisation routine in the LS-SVM toolbox that automatically tuned the parameters through coupled simulated annealing and leave-one-out crossvalidation (De Brabanter et al., 2010).

A possible disadvantage of LS-SVR is that it uses all calibration data as support vectors and thus looses sparseness of the models (Thissen, Üstün, et al., 2004). In order to produce sparser model, pruning techniques have been proposed in which support vectors that contribute less to the model are removed (Suykens et al., 2002). All LS-SVR calculations were performed using the matlab functions in the free LS-SVM toolbox v1.7 (De Brabanter et al., 2010).

2.4.5. Model interpretation

As outlined in section 2.4.1, PLSR models can be interpreted from plotting the regression coefficients (b-coefficients), and a larger absolute value indicates a greater contribution from that specific wavelength to the regression model. While PLSR models are considered sufficiently transparent to enable interpretation, the case is different for the SVM-based methods. With the kernel-based transformation into a high-dimensional feature space, connection with the original input variables is lost and interpretation of the model is rendered complicated. Hence, SVR is mainly applied as a black box and no effort is put into explaining the model structure (Hernández et al., 2009). There is, however, some information in the support vectors and their corresponding support values that can be used for interpretation. This study used an approach proposed by Üstün et al. (2007), in which the inner product of the support vector matrix and the support value vector (α) is plotted and interpreted in a similar manner as the PLSR b-coefficients. The resulting vector (P) has one value per spectral band, and the P-values for the spectral wavelength X is the sum of all support vector variables at that spectral band multiplied by their respective support values:

$$X_1 * \alpha_1 + X_2 * \alpha_2 \ldots X_n * \alpha_n = P_X \qquad (8)$$

where $X_{1\ldots n}$ are support vector variables, and $\alpha_{1\ldots n}$ their corresponding support values. The PLSR b-coefficients and the SVR P-values were subsequently normalised through division by their standard deviations, and then compared with the original wavelength bands. The standard deviation of the weight vector is sometimes used as a threshold to single out the wavelengths that are most important for the model (Bian et al., 2010; Gomez et al., 2008). In this case, one and a half

standard deviation was an appropriate threshold value. The models used for interpretation were calibrated using all available samples.

2.5. Constructing nutrient maps

For successfully modelled biochemicals, maps were created using the regression and transformation method yielding the lowest RMSE. These were generated in MATLAB (The MathWorks, 2010), and the full dataset was used to calibrate the model before applying it on each map pixel. The biochemical content is only shown for pixels with a clear mangrove vegetation spectrum. All other land-cover types, shrimp ponds, lowland non-mangrove forests and mud flats were masked out. Also, mangrove pixels with strong elements of roots, mud or water were eliminated in order to only apply the model on pixels with a comparatively dense mangrove canopy. The separation between mangrove and non-mangrove pixels was made using ISODATA unsupervised classification in ENVI 4.7 (ITT Visual Information Solutions, 2009).

2.6. General workflow of the methodology

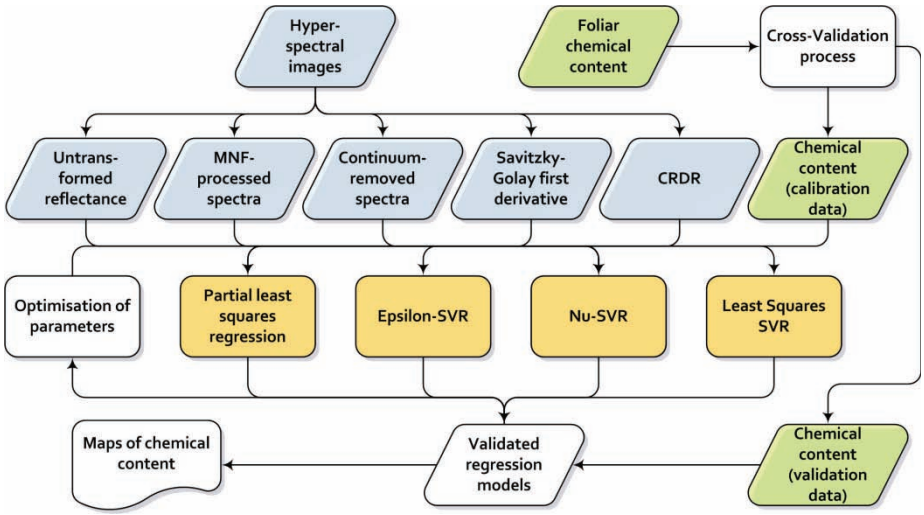

Figure 6: General workflow of the methodology.

3. Results and discussion

"Statistics is the grammar of science"
Karl Pearson (1857–1936)

3.1. Preliminary analysis

For better model performance, a few outliers were removed from the datasets. When validated, outliers bring down prediction results of the model, and outliers in the calibration set are detrimental to the quality of the predictor. Outliers (four in Mahakam, three in Berau) were identified by matching the predicted and measured chemical content in a graph. Figure 7 illustrates the effect of removing one extremely detrimental outlier (M0606). The divergent nutrient content of these outlier samples may have been caused by pixel/plot mismatch, or if the collected leaves were not representative of the sample plot. In the case of M0606, it was later found that it probably was a pixel/plot mismatch.

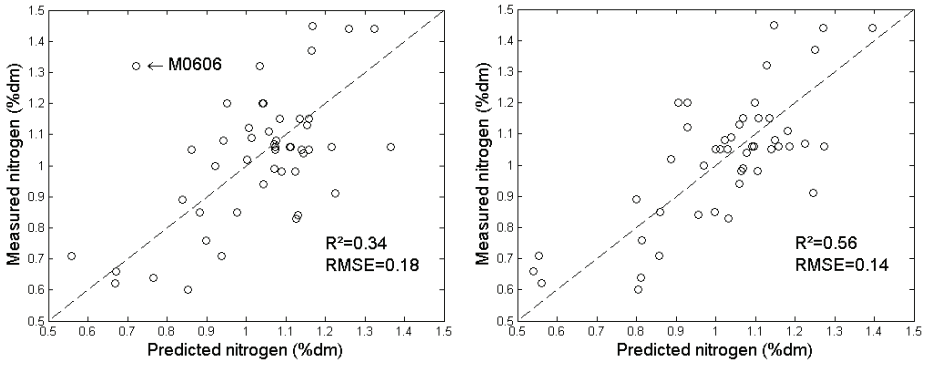

Figure 7: Model results for the Mahakam dataset including the outlier M0606 (left graph), and results for the same dataset after removal of M0606 (right graph).

Table 3 shows the number of samples and statistics for the different chemicals in weight percent of dried matter (%dm). The coefficient of variation is the ratio of the standard deviation to the mean, and is a dimensionless measure of the dispersion within the sample set. The statistics indicate that phosphorus, despite its importance, is a very small component of leaf tissue with mean values at 0.09-0.10 %dm. This is one reason for why it is difficult to estimate its content from the spectral reflectance (N.M. Knox et al., 2010).

Table 3: Sample statistics.

Chem.	Study area	No. of samples	Range (%dm)	Mean (%dm)	Standard deviation (%dm)	Coefficient of variation (%)
N	Berau	74	0.66 - 2.30	1.09	0.29	26.6
	Mahakam	47	0.60 - 1.45	1.02	0.21	20.3
P	Berau	74	0.02 - 0.29	0.09	0.06	64.0
	Mahakam	47	0.07 - 0.16	0.10	0.02	20.7
K	Berau	74	0.24 - 1.45	0.67	0.24	35.5
	Mahakam	47	0.36 - 0.61	0.50	0.06	12.3
Ca	Berau	74	0.03 - 6.47	2.07	1.37	66.2
	Mahakam	47	0.28 - 1.48	0.75	0.38	50.2
Mg	Berau	74	0.10 - 0.38	0.29	0.07	23.8
	Mahakam	47	0.03 - 0.39	0.29	0.09	31.1
Na	Berau	74	0.23 - 0.90	0.74	0.17	22.8
	Mahakam	47	0.23 - 1.33	0.77	0.30	39.4

It is important to note that the Mahakam samples were collected and analysed in 2009, and the Berau samples in 2010. Differences in calibration of the instruments at the chemical laboratory, and temporal climatic factors, such as differences in the amount of rainfall between the two years, may therefore affect the measured chemical contents. The samples are also not completely representative of the whole area since they were concentrated to specific transects. It is therefore not possible to draw conclusions on differences between the two study areas based on these numbers.

Table 4 shows nitrogen prediction results using all available wavelength bands. Overall, the choice of spectral transformation technique had a major impact on model performance. All transformation techniques improved the results compared to the untransformed reflectance, and best results were obtained using CRDR. The higher performance of CRDR goes in line with the results of Mutanga et al.(2004) and Kawamura et al.(2009). Continuum-removal applied on the full spectra can thus successfully remove the background trend of the reflectance spectra which has little or no relationship with the biochemical content. Spectra are thereby normalised to a common base-line. By then using the derivative of the continuum-free spectra, absorption features associated with nitrogen are further enhanced.

Table 4: Nitrogen prediction results using all spectral bands. All models were validated using leave-one-out crossvalidation. The parameter settings presented are the median settings for all validation iterations.

		Nitrogen Berau			Nitrogen Mahakam		
Regression	Transformation	R^2cv	RMSEcv	Parameters	R^2cv	RMSEcv	Parameters
ε -SVR	none	0.269	0.248	c=5,eps=0.11,nSV=39	0.263	0.178	c=2,eps=0.11,nSV=24
	MNF-processed	0.326	0.251	c=5,eps=0.11,nSV=39	0.280	0.176	c=3,eps=0.11,nSV=24
	Continuum-removed	0.490	0.210	c=5,eps=0.11,nSV=39	0.433	0.155	c=5,eps=0.11,nSV=21
	First derivative	0.441	0.218	c=5,eps=0.11,nSV=42	0.514	0.144	c=5,eps=0.11,nSV=20
	CRDR	0.533	0.199	c=5,eps=0.11,nSV=36	0.510	0.144	c=4,eps=0.11,nSV=21
ν-SVR	none	0.289	0.245	c=5,nu=0.6,nSV=48	0.357	0.166	c=5,nu=0.8,nSV=39
	MNF-processed	0.373	0.248	c=5,nu=0.7,nSV=53	0.323	0.170	c=5,nu=0.8,nSV=39
	Continuum-removed	0.457	0.215	c=5,nu=0.3,nSV=32	0.448	0.153	c=5,nu=0.4,nSV=31
	First derivative	0.446	0.217	c=5,nu=0.4,nSV=46	0.437	0.155	c=5,nu=0.4,nSV=33
	CRDR	0.516	0.203	c=5,nu=0.4,nSV=43	0.523	0.142	c=4,nu=0.6,nSV=32
LS-SVR	none	0.293	0.249	gam=3.6,sig2=45	0.410	0.163	gam=161449.3,sig2=345686
	MNF-processed	0.539	0.198	gam=44.6,sig2=371	0.363	0.169	gam=5340.6,sig2=118604
	Continuum-removed	0.450	0.215	gam=19.8,sig2=1085	0.522	0.143	gam=8748.6,sig2=205233
	First derivative	0.421	0.221	gam=6.8,sig2=304	0.487	0.148	gam=232.7,sig2=19341
	CRDR	0.554	0.194	gam=4.1,sig2=219	0.521	0.144	gam=585.7,sig2=32438
PLSR	none	0.546	0.199	no. of components=8	0.321	0.179	no. of components=5
	MNF-processed	0.548	0.197	no. of components=8	0.429	0.160	no. of components=5
	Continuum-removed	0.557	0.196	no. of components=8	0.612	0.130	no. of components=5
	First derivative	0.487	0.213	no. of components=8	0.529	0.147	no. of components=4
	CRDR	0.575	0.191	no. of components=7	0.654	0.122	no. of components=5

3.2. Relative importance of spectral wavelengths

First, nitrogen was modelled using all available bands in order to find out which combination of regression technique and transformation method to use during model interpretation. Due to the higher performance of CRDR-based models, these models were then used for identifying the relative importance of the spectral bands. In figure 8, patterns for the LS-SVR and PLSR coefficients follow each other closely, indicating that the SVR P-vector does, indeed, contain similar information as the PLSR b-coefficients and can be interpreted in a similar manner.

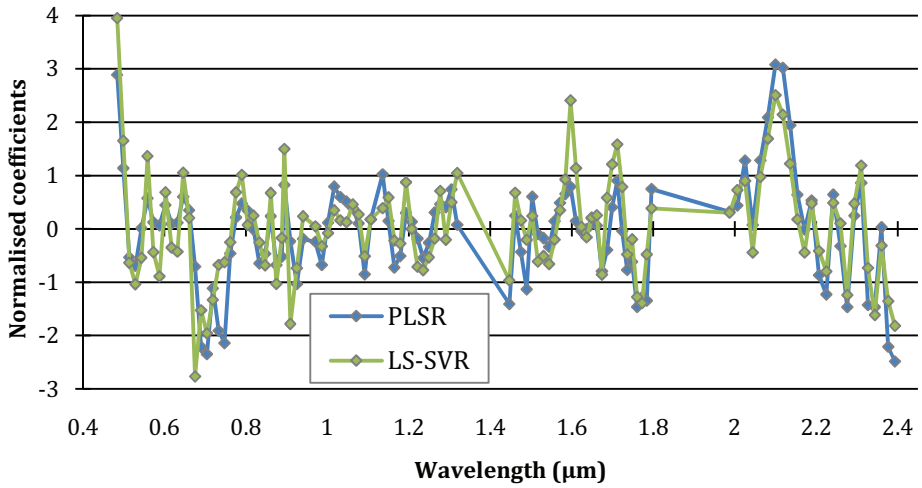

Figure 8: Relative importance of spectral bands for estimating N in Berau using CRDR transformed reflectance. The coefficients were normalised through division by their respective standard deviations.

Due to covariance between N content and other related genera-specific biochemical or structural properties of mangroves, models are derived from a mix of relationships, and only partially from general nitrogen related absorption features. In an attempt to reduce links with genera in the coefficients, also information on genera for each sample was included when calibrating the model (figure 9). Many of the relationships directly attributed to genera were thereby concentrated in the coefficients for the added genera information, and coefficients for the spectral data became less influenced by these factors.

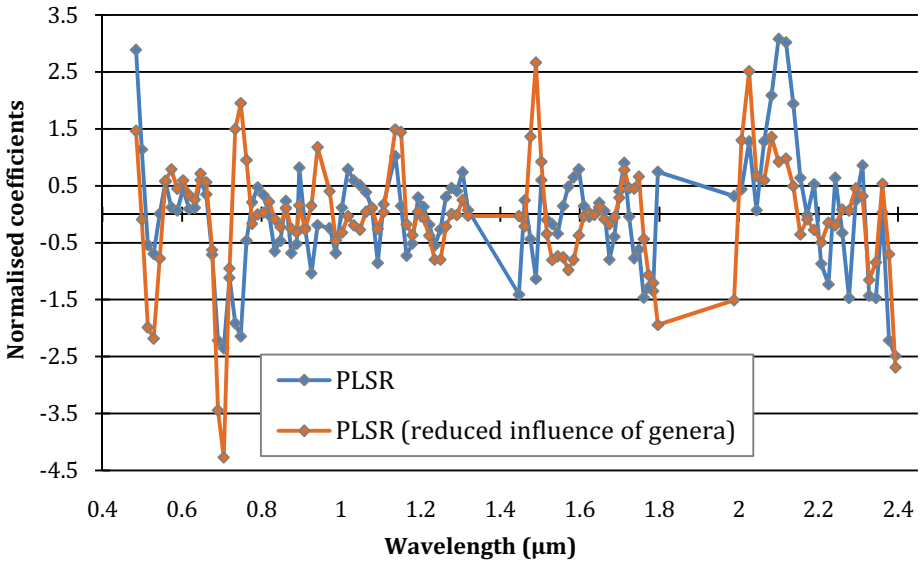

Figure 9: Relative importance of spectral bands for a model derived solely from HyMap data and a model that also included information on mangrove genera. Both models were based on CRDR transformed data for Berau.

Notable differences in the coefficients with less influence of genera are a more pronounced influence of chlorophyll absorption around 0.5 µm, the red edge 0.67-0.75 µm, and protein absorption at 1.5 µm.

Table 5: Relative importance of wavelengths influenced by chlorophyll (0.4-0.8 µm).

	Relative importance	Rel. importance (red. infl. of genera)
Berau	25%	34%
Mahakam	20%	28%

According to the PLSR coefficients, the models attributed 20-25% of the total sum of coefficients to wavelengths affected by chlorophyll. These numbers increased to 28-34% when the influence of genera was reduced. The link between chlorophyll and nitrogen is relatively weaker in the Mahakam models, which, in theory, could indicate a lower level of nitrogen limitation in that area. Also, the wavelengths of highest importance were located further away from the chlorophyll absorption maxima in the case of Mahakam, suggesting a higher degree of saturation.

Table 6: Wavelengths of importance for estimating nitrogen (both Berau and Mahakam).

Wavelengths (µm)	Wavelengths in literature (µm)	Compound	Reference
0.48-0.60	0.43, 0.46, 0.64, 0.66	Chlorophyll a and b	(Curran, 1989)
0.67-0.75	0.68, 0.75	Chlorophyll, "the red edge"	(Cho & Skidmore, 2006; Curran et al., 2001; Martin et al., 1997)
0.91	0.91	Protein	(Curran, 1989)
1.13	1.12	Lignin	(Curran, 1989)
1.32-1.44	1.36, 1.42	Protein, lignin	(Card et al., 1988; Fourty et al., 1996; N. M. Knox et al., 2010)
1.48-1.50	1.50, 1.51	Protein, nitrogen	(Curran, 1989; Curran et al., 2001)
1.60	1.61	-	(Serrano et al., 2002)
1.67-1.71	1.69	Lignin, starch, protein, nitrogen	(Curran, 1989)
1.78-2.02	1.94, 1.98	Protein, nitrogen, lignin	(Curran, 1989)
2.08-2.14	2.08, 2.11, 2.13	Protein	(Card et al., 1988; Curran, 1989)
2.18-2.22	2.18, 2.24	Protein, nitrogen	(Curran, 1989)
2.28-2.30	2.29, 2.30	Protein, nitrogen	(Curran, 1989; Martin et al., 1997)
2.34-2.39	2.35, 2.36	Protein, nitrogen	(Card et al., 1988; Curran et al., 2001)

Table 6 shows the identified wavelengths of highest influence with references to previously identified absorption features of nitrogen. The bands were selected based on both the regular models and models with reduced genera influence. In the visible region, important wavelengths were located in two blocks 0.48-0.60 µm and 0.67-0.75 µm, indicating that wavelengths of highest chlorophyll absorption in the red (0.64-0.66 µm) were saturated and the amount of chlorophyll was best estimated from wavelengths on the edges to green and infrared. This saturation effect is common for absorption features linked to chlorophyll, as well as proteins and other compounds, and means that wavelengths where the absorption is less strong are

often more strongly related to biochemical content than wavelengths at the absorption maxima (Curran, 1989; Kokaly, 2001).

In the short-wave infrared (SWIR) region from 1.4 to 2.5 µm, nitrogen is estimated from absorption features of proteins. The effects of absorption features are generally spread out, and not concentrated to specific wavebands. Most information seems to be held on the slopes before and after absorption features and not in the wavelengths of maximum absorption. This could indicate saturation, but is probably also an effect of using CRDR, in which five bands are used to calculate the derivative at each wavelength. Trends thereby become clear on the slopes, but may be inconclusive at bands where the reflectance curve changes direction.

The wavebands of high importance for the models could usually, but not always, be linked to previously identified absorption features of nitrogen. The band at 1.13 µm was of relevance for both Berau and Mahakam models, but is only known in the literature to be related to lignin. Lignin does not contain nitrogen, but it has been known to correlate with the availability of nitrogen in temperate forests by determining decomposition and nitrogen mineralisation rates of litter (Wessman et al., 1988).

Based on the PLSR and SVR coefficients, the most influential bands around the absorption features were selected to produce models less affected by redundant information. In the case of highly informative bands close to each other in the spectra, a few test runs were carried out to ensure there were no detrimental effects from multicollinearity. The selected bands are presented in table 7.

Table 7: Selected wavelengths (µm) used in the final nitrogen models.

Berau	0.484, 0.705, 0.909, 1.489, 1.597, 1.712, 1.796, 2.025, 2.082, 2.118, 2.225, 2.277, 2.344, 2.393
Mahakam	0.558, 0.588, 0.733, 0.909, 1.136, 1.447, 1. 76, 1.674, 1.784, 2.118, 2.189, 2.294, 2.361, 2.393

3.3. Nitrogen prediction results

Table 8: Nitrogen prediction results from using the selected CRDR bands in table 7.

	Nitrogen Berau			Nitrogen Mahakam		
Regression	R^2cv	RMSEcv	nRMSEcv	R^2cv	RMSEcv	nRMSEcv
ε -SVR	0.647	0.173	15.9%	0.657	0.121	11.9%
ν-SVR	0.675	0.167	15.3%	0.674	0.118	11.6%
LS-SVR	0.672	0.166	15.2%	0.692	0.115	11.2%
PLSR	0.566	0.193	17.7%	0.657	0.121	11.9%

The best performing model for Berau (R^2=0.67, RMSE=0.17, nRMSE=15%) and for Mahakam (R^2=0.69, RMSE=0.12, nRMSE=11%), both show successful estimations of foliar nitrogen. The lower performance of the Berau model is probably due to the poor image quality of that area, and because of the time gap of one year between image recording and sample collection.

While the results of PLSR show little or no improvement from narrowing down the number of bands, SVR improves greatly. The performance of SVR is thus highly susceptible to multicollinearity and redundant information in the independent variables, which also was noted by Wang et al. (2010). The best performing model for Berau and Mahakam were both based on LS-SVR. Based on theoretical comparisons, the main advantage of LS-SVR over ε-SVR and ν-SVR is the computationally faster algorithm (Shmilovici, 2005). In practice, however, LS-SVR has also in other cases shown higher performance. This is probably because the algorithm can be trained more efficiently (Chauchard et al., 2004), and is easier to optimise accurately (Hernández et al., 2009).

The generally higher performance of SVR compared to PLSR has been noted in previous studies (Thissen, Pepers, et al., 2004), and is often attributed to its ability to map non-linear relationships. However, there are also cases in which PLSR has outperformed SVR (Shah et al., 2010). These differences are likely to depend on the degree of non-linearity in the relations, the degree of multicollinearity and noise in the independent variables, and how accurately the SVR parameters can be tuned. In this study, the tuning process of ε-SVR and ν-SVR proved to be difficult and time-consuming. Although the grid-search used for parameter tuning was automatic, it took time to learn how to properly set the intervals and boundaries of the grid-search. LS-SVR was far easier to apply in this respect, due to the built-in optimisation routine in the LS-SVM toolbox.

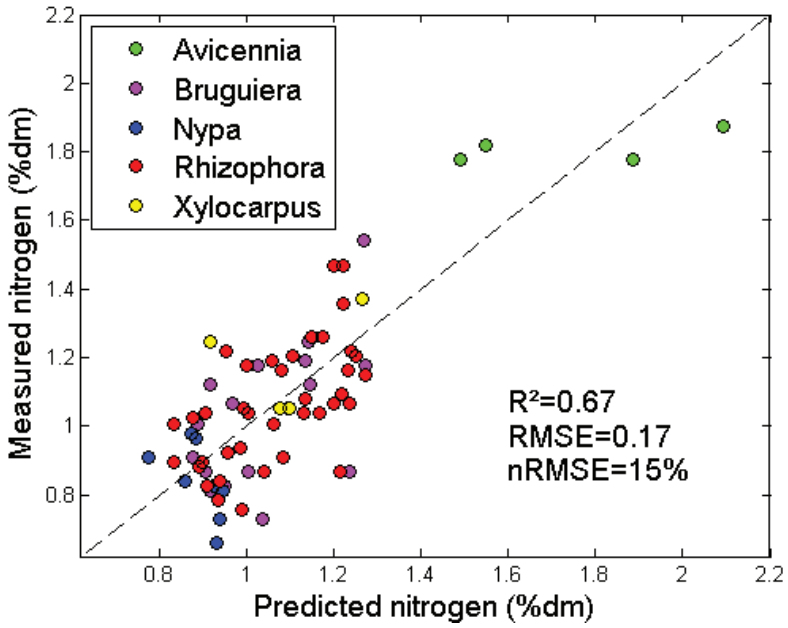

Figure 10: Nitrogen prediction for the Berau dataset, using LS-SVR and CRDR.

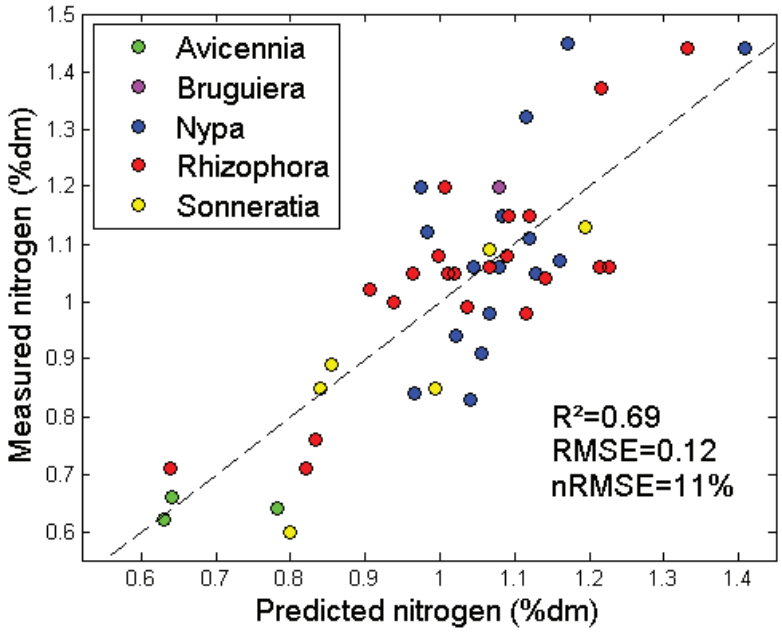

Figure 11: Nitrogen prediction for the Mahakam dataset, using LS-SVR and CRDR.

Figures 10 and 11 show predictions of the highest performing models for each study area. Clearly, the ranges of nitrogen content vary between the different genera. Rhizophora, the most common genera in both areas, contain both higher and lower values of measured nitrogen. This caters for strong relationships also for within-genera models. A model based solely on Rhizophora samples could thereby also predict nitrogen with high performance (R^2=0.64, RMSE=0.12, Mahakam dataset). Nypa and Avicennia are more clustered, resulting in poor within-genera performance. Interestingly, Avicennia in Berau have all high nitrogen content, while in Mahakam they are clustered in the lower range.

When extending studies from single species to multiple species environments, precision generally increases and the accuracy decreases. The greater range of biochemical content, associated with a larger variety of species, makes it easier to find a relationship which may be partly based on covariance with related factors such as vegetation structure of the different species. The accuracy is usually higher in single species studies because those models can adapt more closely to spectral characteristics of the particular species.

3.4. Predictions of biochemicals other than nitrogen

Table 9: Model results for biochemicals other than nitrogen. Results shown are for the best performing models in terms of lowest RMSE.

	Chemical	Regression	Transformation	R^2	RMSE	nRMSE
Berau	P	ν-SVR	None	0.218	0.049	56.6%
	K	LS-SVR	Continuum-removed	0.309	0.196	29.3%
	Ca	LS-SVR	Continuum-removed	0.395	1.067	51.5%
	Mg	LS-SVR	CRDR	0.678	0.039	13.4%
	Na	PLSR	CRDR	0.851	0.065	8.8%
Mahakam	P	LS-SVR	First derivative	0.046	0.020	21.3%
	K	ν-SVR	First derivative	0.300	0.051	10.2%
	Ca	LS-SVR	CRDR	0.266	0.322	42.6%
	Mg	ν-SVR	Continuum-removed	0.457	0.068	23.0%
	Na	ε -SVR	First derivative	0.166	0.275	35.6%

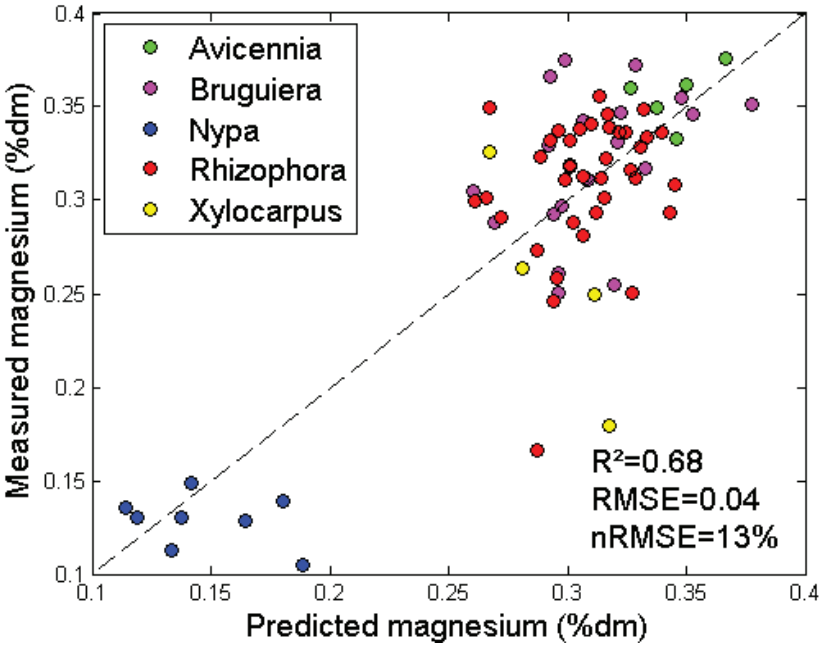

Figure 12: Magnesium prediction for the Berau dataset.

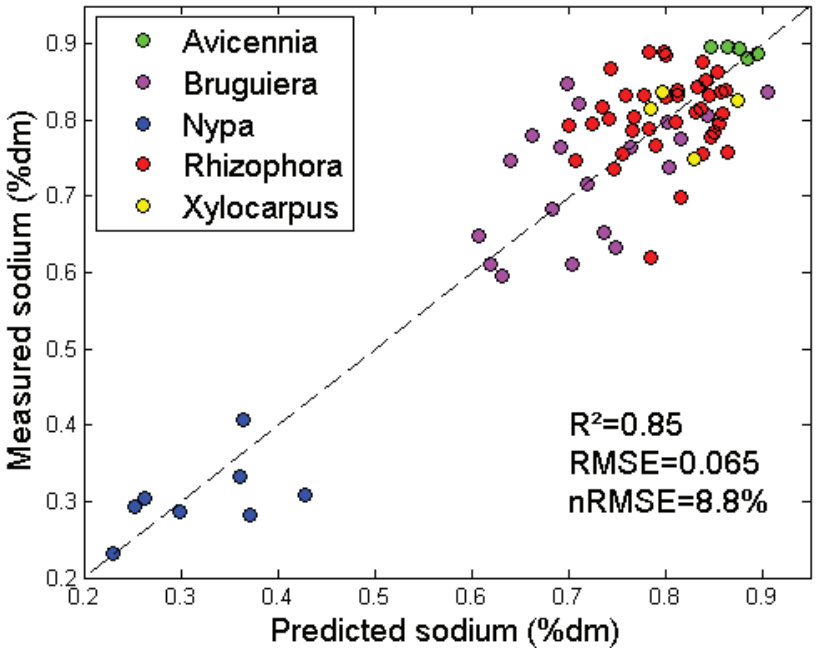

Figure 13: Sodium prediction for the Berau dataset.

Results for biochemicals other than nitrogen are generally poor. While the nitrogen content in leaves can be traced through the absorption of chlorophyll and proteins, the other examined biochemicals are less traceable because their content is not related to optically active elements in the leaves. Although previous studies sometimes have claimed to model these biochemicals, found relationships are usually either tied to the composition of species (Ferwerda et al., 2007), or based on site-specific correlation with more spectrally visible biochemicals such as nitrogen (Porder et al., 2005). Those models might be of some use within that specific area, but are not possible to apply in a wider context. Such relationships are of little use when trying to map the complex biochemical variation in mangroves.

Prediction results for magnesium and sodium in Berau are seemingly high. However, graphs of the predicted contents (figures 12 and 13) show that samples are strongly clustered, thus producing artificially high correlations. The within-genera correlations were also found to be much weaker than those for nitrogen, indicating that relationships are formed through genera-specific spectral characteristics such as vegetation structure. The strong link between Na-Mg contents and genera partly reflects the habitats of these species. *Avicennia alba* grows along coastal fringes, frequently inundated by sea water rich in sodium and magnesium ions. *Nypa*, on the other hand, is adapted to grow further from the ocean in more brackish conditions (Sulong et al., 2002), and absorb much lower concentrations of these chemicals.

Figure 14: *Nypa fruticans* (left) is the only palm tree among mangroves. It grows in less saline environments, while *Avicennia alba* (right) has adapted to the most saline habitats close to the ocean.

3.5. Maps of nitrogen content

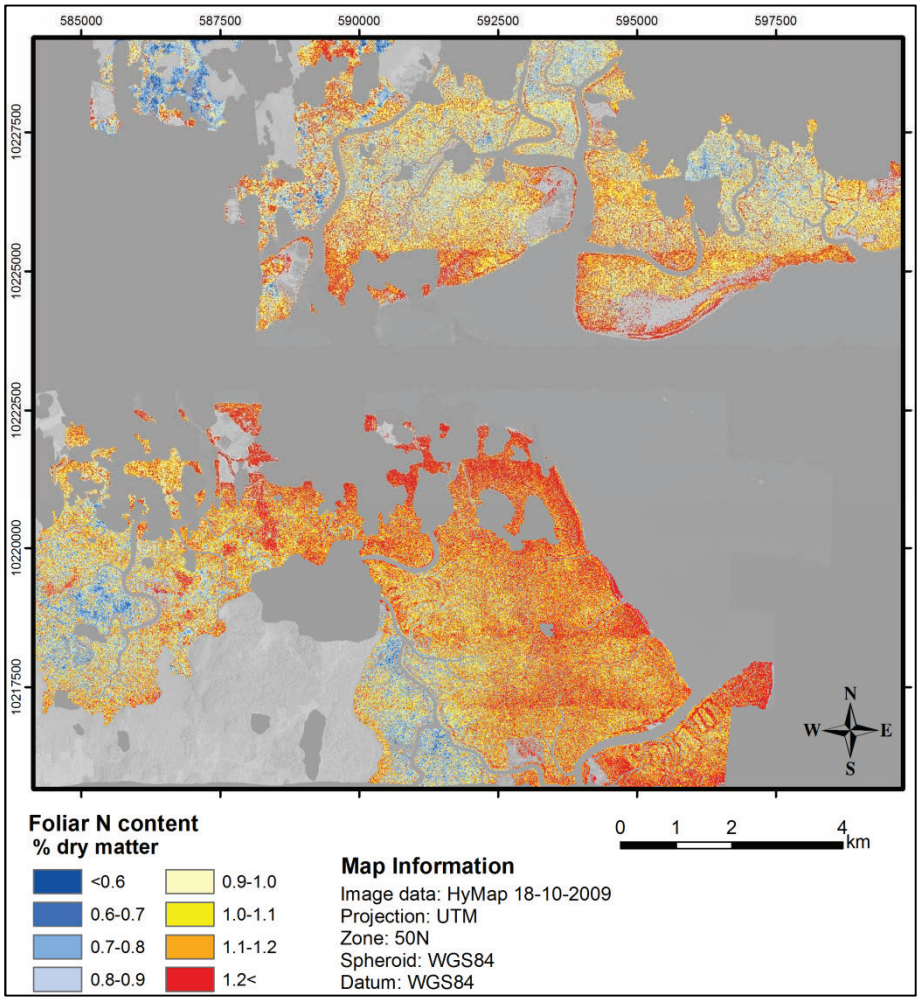

Figure 15: Map of nitrogen content in the Berau study area derived through PLSR using all CRDR bands.

Due to the poor results from P, K, Ca, Mg and Na predictions, only the nitrogen models were deemed powerful enough to generate maps of the study areas. Although the Berau models for magnesium and sodium showed high accuracy and precision, their low within-genera performance makes them unsuitable for biochemical mapping. A sodium map of Berau would thus only show the composition of different genera in the area.

The Berau map shows some horizontal striping that coincides with the flight lines of the aircraft. These artefacts are caused by insufficient atmospheric correction of the Berau images. Striping was even more deteriorating in a previous version of the map. By redoing the MNF-transformation and being much more selective on which bands to invert back, the effect of striping could be greatly reduced. Also, it was found that a map generated using the model of highest performance (LS-SVR on the fourteen most important bands) was more sensitive to striping than a model generated through PLSR using all bands. This is probably related both to a higher susceptibility to noise in the few selected bands, and differences in how the two methods cope with noise. PLSR is known to be able to handle noise well by suppressing it in the extracted latent variables (Wold et al., 2001), and it may therefore be a better option in cases of noisy data. Another alternative could be to combine the two methods. Chauchard et al.(2004) compared the performance of LS-SVR and PLSR on data containing different kinds of noise and found LS-SVR to be highly noise-sensitive. By applying LS-SVR on latent variables (PLS components), they achieved higher performance than with LS-SVR applied on wavelength bands or when using the PLSR method.

Because the map generated using LS-SVR was more affected by striping, the Berau map presented in figure 15 is instead derived from PLSR applied on the full spectra. The general trend of the map is that levels are higher closer to the shore than further inland, suggesting that mangroves are fed with nitrogen from the main river channel. However, for many of the smaller creeks, nitrogen levels seem low close by the creek and higher further away. In a review of previous studies on nutrient dynamics in mangroves, Adame & Lovelock (2011) observed that mangroves sometimes import and sometimes export nitrogen. Significant correlations were found between dissolved N exchange and N concentration in the floodwater as well as the tidal amplitude. Imports were higher in cases of high N concentration in the floodwater, while exports are common when the floodwater has low N concentration. Both import and export cases are enhanced by higher tidal amplitude, which generally occurs closer to the water channels. In the case of Berau, foliar N contents suggest N imports around the main river channel. By the smaller creeks further away from the main river channel, diffusion of nitrogen from sediments to the less nutrient-rich creek water might cause lower foliar N concentrations in surrounding mangroves.

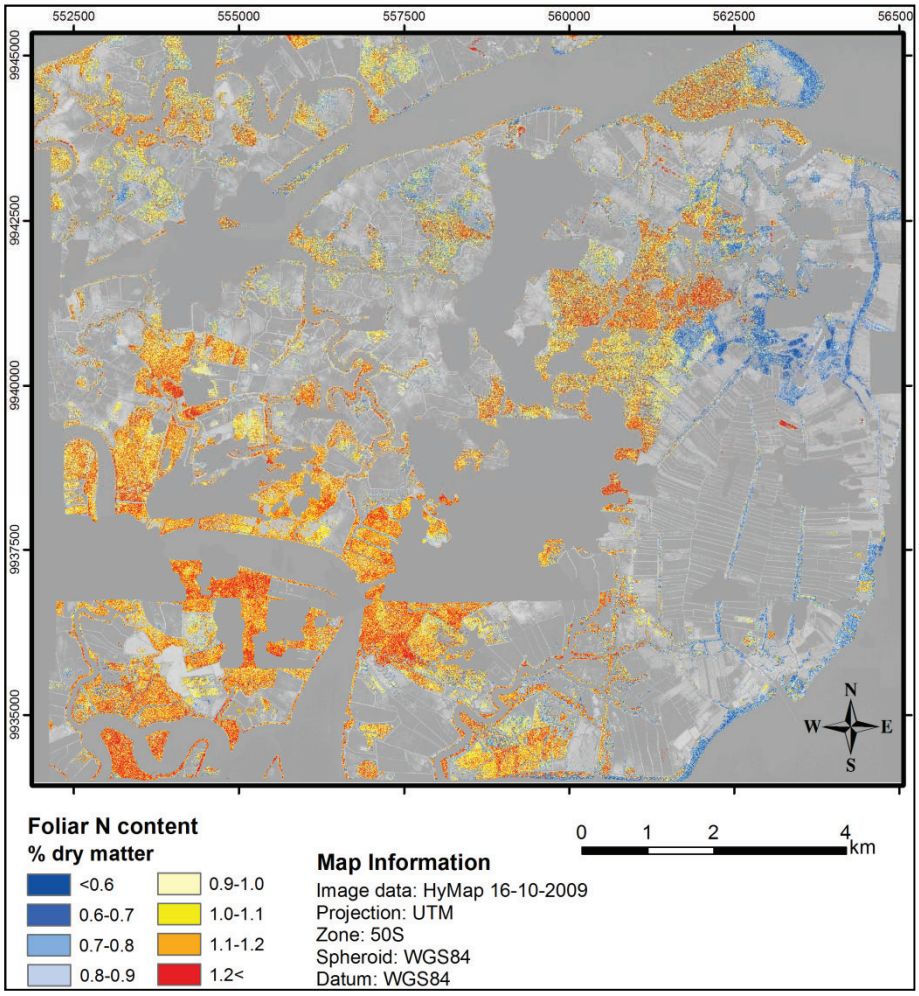

Figure 16: Map of nitrogen content in the Mahakam study area derived through LS-SVR and CRDR, using the selected wavelength bands in table 7.

The Mahakam map shows a pattern of higher nitrogen levels in the west mainly affected by river water, and lower levels in the east, mainly affected by sea water. Unlike in Berau, nitrogen levels seem very low along the coastal fringes. The differences are possibly related to the coastal morphology of the two study areas. The Berau study area is located in a sheltered bay with an archipelago offshore, and may therefore be less exposed to ocean dynamics and influx of nutrient poor seawater than the eastern part of the Mahakam study area.

Mangroves growing further inland are fed with nutrients from the river, and possibly also from the shrimp ponds. However, these results do not show signs of extreme foliar nitrogen values related to anthropogenic disturbances in the delta. Due to a lack of information on the status of the shrimp ponds and the quality of the water, an attempt at interpretation is bound to be speculative. It may, however, be that the shrimp ponds are mainly extensively managed, or simply that the level of confinement is low. Low confinement, in this respect, means that the capacity of the ecosystem to change its water is high enough to prevent large amounts of nutrients leaking from the shrimp ponds to accumulate in the surrounding area (Martin, 2011).

It is important to note that no certain conclusions can be drawn only based on the derived maps. The maps are only as reliable as the models they are based on, and the models rely on to which degree the ground samples capture the variation in the study areas. One weakness is the low variety in the sampled *Avicennia spp*. As it turned out, all *Avicennia* samples in Mahakam had low nitrogen content, creating a risk of all *Avicennia* throughout the area being categorised as low in nitrogen.

4. Conclusions and recommendations

"It is not the possession of truth, but the success which attends the seeking after it, that enriches the seeker and brings happiness to him."

Max Planck (1858-1947)

4.1. Conclusions

This study has demonstrated the possibility to accurately estimate nitrogen in mangroves using airborne hyperspectral data and empirical modelling. The highest performing nitrogen prediction model for Berau (R^2=0.67, RMSE=0.17, nRMSE=15%), and for Mahakam (R^2=0.69, RMSE=0.12, nRMSE=11%) both show encouraging results. The content of P, K, Ca, Mg and Na proved much more difficult to estimate because the variation of these chemicals cannot be tied to optically active compounds in the foliage.

The performance of four different regression techniques, ε-SVR, ν-SVR, LS-SVR, and PLSR, were evaluated. LS-SVR yielded the highest accuracy, and was found to be a highly efficient tool in biochemical modelling. It is, however, necessary to remove collinearity and redundant information in the data for optimal performance. In the final LS-SVR models, only the fourteen most informative wavelength bands were used to derive the model. These were identified using the relative importance of the bands, reflected in the regression coefficients. It was demonstrated that the SVR P-vector, derived from the support vectors and their corresponding support values, contains similar information as the PLSR regression coefficients, and can be interpreted in a similar manner. PLSR can handle multicollinearity and noise better than LS-SVR, and should be preferred in analysis of noisy or collinear variables.

Different spectral transformation methods were compared with respect to their influence on the performance of the predictive models. Continuum-removed derivative reflectance (CRDR) proved to be the most efficient transformation method at enhancing absorption features related to nitrogen.

One of the research objectives of this study is to find ways to counteract the influence of varying LAI, and covariance with the vegetation structure of different species. That was made in the following ways:

- In order to reduce the influence of varying LAI, I was particularly careful when selecting which pixels to represent each sample plot. Pixels with elements of mud or roots were avoided and only comparatively pure vegetation pixels were included. Furthermore, in the process of making the

nitrogen maps I was careful in filtering out pixels with less pure vegetation spectra. These steps should reduce contamination from pixels with very low LAI in the derived maps.

- When analysing which bands are most important to predict nitrogen, I was especially interested in bands related to the within-genera variation of nitrogen. By adding information on genera to the calibration data, it was possible to reduce the influence of genera in the regression coefficients for the hyperspectral data and thereby identify wavelength bands of particular importance for modelling the within-genera variability.

The ability to map nitrogen from remote sensing data can prove important when analysing ecosystem processes and the complex patterns of nitrogen fluxes in mangroves. Nitrogen maps for the two study areas were derived using the established models. These maps give indications of the general patterns of foliar nitrogen, and these patterns may reveal links to natural or anthropogenic factors influencing the nitrogen dynamics in the study areas. When attempting to interpret the maps, possible links to species composition, tidal amplitude, nitrogen concentration in the floodwater, and the coastal morphology of the study areas were found. No clear signs of excessive nitrogen levels related to anthropogenic sources were identified.

4.2. Summary of answers to research questions

This section contains a brief answer to each of the three research questions.

Question: To which degree can foliar N, P, K, Ca, Mg and Na concentrations be estimated using airborne HyMap images and regression techniques?

Answer: N could be estimated to within 11-15% of its mean content, as shown in table 8. Estimations of P (rel. error 21-57%), K (rel. error 10-29%), Ca (rel. error 43-52%), Mg (rel. error 13-23%), and Na (rel. error 9-36%) are shown in table 9. These are generally poor, or show a strong covariance with genera.

Question: Which regression technique shows the highest explained variability (R^2) and lowest root-mean-squared error (RMSE)?

Answer: These are evaluated based on the highest performing predictive models for nitrogen, shown in table 8. For the Berau dataset the highest performing models were based on LS-SVR (R^2=0.67, RMSE=0.17), and ν-SVR (R^2=0.68, RMSE=0.17). For Mahakam dataset the highest performing model was based on LS-SVR (R^2=0.69, RMSE=0.12).

Question: Can the models be explained? That is, which bands are most important and can these bands be related to known biochemical absorption features?
Answer: Most of the highly influential wavelength bands can be related to previously identified absorption features, as shown in table 6. However, the impact of absorption features were spread out over several bands and were usually not strongest at the wavelength of highest absorption. Not all influential bands could be related to known absorption features; the band at 1.13 µm is known to be sensitive to the content of lignin, but not nitrogen.

4.3. Limitations

This section mentions some of the limitations of the conducted study.

- Due to the known absorption features related to nitrogen, and its importance in physiological processes, more effort was put into modelling nitrogen than the other biochemicals. It is likely that prediction results for P, K, Ca, Mg, and Na would have improved from narrowing down the number of used bands, as in the case of nitrogen. That was never done because of the evidently poor within-genera prediction results of those chemicals.

- The narrowing down of wavelength bands was necessary due to the inability of SVR to handle collinearity and redundant information in the full spectra. That was, however, not known at the start of the study and no proper methodology was developed for how to best do this step. Stepwise multiple linear regression may, for instance, have been a useful tool when narrowing down the bands that also would have given the significance of each wavelength band.

4.4. Recommendations

- LS-SVR proved to be an efficient modelling tool that was easy to apply. One major factor that has hampered the use of SVR-based methods in research during the last decade is a lack of easy-to-use SVR tools. Especially, the tuning process of the regression parameters has been difficult. The LS-SVM toolbox v1.7 (De Brabanter et al., 2010) provides many functions that makes LS-SVR easy to apply in research. The recent optimisation routine based on Coupled Simulated Annealing (CSA) is of particular importance.

- In future applications of SVR in biochemical modelling, it is important to find proper methods for narrowing down the number of bands. This may be done through stepwise multiple linear regression, perhaps in combination with analysis of the regression coefficients, or by utilising vegetation indices.

Another way to reduce the number of bands that also improves its ability to cope with noise is to apply SVR on latent variables, as shown by Chalimourda et al. (2004).

- Continuum-removed derivative spectra (CRDR) was, to my knowledge, first described by Mutanga et al. (2004), and has not been used often in biochemical modelling despite having shown promising results in the few studies that have employed it. This study further indicates that continuum-removal can successfully be applied on the full spectra and that the derivative of the continuum-removed spectra further enhances absorption features. In this study, I applied continuum removal separately on two parts of the spectra (0.45-1.45 µm, and 1.45-2.43 µm), in order to make the continuum line follow the general trend of the vegetation spectra more closely. This approach seemed to improve the prediction results, and I recommend it to be further investigated in future studies.

4.5. Future directions

Given the rapid technological advancements in the last decades, it seems inevitable that nitrogen will increasingly be estimated using space-based sensors. A few studies have already used space-borne Hyperion data to predict nitrogen with promising results (Smith et al., 2003). More research is needed to advance beyond site-specific studies and look at the global level. Martin et al. (2008) took one step in that direction by merging many local studies and trying to find a more generalised empirical model that is applicable over a range of landscapes. However, empirical models will always be dependent on which sites and species that are included in the calibration set. If an empirical approach is pursued at the global level, it would be necessary to collect an enormous amount of calibration data. Instead, it would be more advantageous to use the relationships found in empirical studies and incorporate them into more general and portable physical models or vegetation indices.

5. References

Abdi, H. (2010). Partial least squares regression and projection on latent structure regression (PLS Regression). *Wiley Interdisciplinary Reviews: Computational Statistics, 2*(1), 97-106.

Aburto-Oropeza, O., Ezcurra, E., Danemann, G., Valdez, V., Murray, J., & Sala, E. (2008). Mangroves in the Gulf of California increase fishery yields. *Proceedings of the National Academy of Sciences, 105*(30), 10456.

Adame, M., & Lovelock, C. (2011). Carbon and nutrient exchange of mangrove forests with the coastal ocean. *Hydrobiologia, 663*(1), 23-50.

Alongi, D. M. (2008). Mangrove forests: Resilience, protection from tsunamis, and responses to global climate change. *Estuarine, Coastal and Shelf Science, 76*(1), 1-13.

Alongi, D. M. (2011). Early growth responses of mangroves to different rates of nitrogen and phosphorus supply. *Journal of Experimental Marine Biology and Ecology, 397*(2), 85-93.

Asner, G. P. (1998). Biophysical and Biochemical Sources of Variability in Canopy Reflectance. *Remote sensing of environment, 64*(3), 234-253.

Asner, G. P. (2008). Hyperspectral remote sensing of canopy, chemistry, physiology, and biodiversity in tropical rainforests. In M. Kalacska & G. Sanchez-Azofeifa (Eds.), *Hyperspectral remote sensing of tropical and subtropical forests* (pp. 261-296). Boca Raton, FL, USA: CRC Press.

Asner, G. P., & Martin, R. E. (2008). Spectral and chemical analysis of tropical forests: Scaling from leaf to canopy levels. *Remote sensing of environment, 112*(10), 3958-3970.

Atzberger, C., Guérif, M., Baret, F., & Werner, W. (2010). Comparative analysis of three chemometric techniques for the spectroradiometric assessment of canopy chlorophyll content in winter wheat. *Computers and Electronics in Agriculture, 73*(2), 165-173.

Baret, F., Clevers, J. G. P. W., & Steven, M. D. (1995). The robustness of canopy gap fraction estimates from red and near-infrared reflectances: A comparison of approaches. *Remote sensing of environment, 54*(2), 141-151.

Barton, C. V. M., & North, P. R. J. (2001). Remote sensing of canopy light use efficiency using the photochemical reflectance index: Model and sensitivity analysis. *Remote sensing of environment, 78*(3), 264-273.

Bian, M., Skidmore, A. K., Schlerf, M., Fei, T., Liu, Y. F., & Wang, T. J. (2010). Reflectance spectroscopy of biochemical components as indicators of tea, Camellia Sinensis, quality. *Photogrammetric Engineering and Remote Sensing, 76*(12).

Boto, K. G., & Robertson, A. I. (1990). The relationship between nitrogen fixation and tidal exports of nitrogen in a tropical mangrove system. *Estuarine, Coastal and Shelf Science, 31*(5), 531-540.

Bouillon, S., Borges, A., Castaneda-Moya, E., Diele, K., Dittmar, T., Duke, N., et al. (2008). Mangrove production and carbon sinks: A revision of global budget estimates. *Global Biogeochemical Cycles, 22*(2).

Cao, L., & Tay, F. (2004). Support vector machine with adaptive parameters in financial time series forecasting. *Neural Networks, IEEE Transactions on, 14*(6), 1506-1518.

Card, D. H., Peterson, D. L., Matson, P. A., & Aber, J. D. (1988). Prediction of leaf chemistry by the use of visible and near infrared reflectance spectroscopy. *Remote sensing of environment, 26*(2), 123-147.

Chalimourda, A., Schölkopf, B., & Smola, A. J. (2004). Experimentally optimal [nu] in support vector regression for different noise models and parameter settings. *Neural Networks, 17*(1), 127-141.

Chang, C., & Lin, C. (2001). LIBSVM: a library for support vector machines: Citeseer.

Chapelle, O., Haffner, P., & Vapnik, V. (2002). Support vector machines for histogram-based image classification. *Neural Networks, IEEE Transactions on, 10*(5), 1055-1064.

Chauchard, F., Cogdill, R., Roussel, S., Roger, J. M., & Bellon-Maurel, V. (2004). Application of LS-SVM to non-linear phenomena in NIR spectroscopy: development of a robust and portable sensor for acidity prediction in grapes. *Chemometrics and Intelligent Laboratory Systems, 71*(2), 141-150.

Childers, D. L., Day, J. W., & McKellar, H. N. (2002). Twenty More Years of Marsh and Estuarine Flux Studies: Revisiting Nixon (1980). In M. P. Weinstein & D. A. Kreeger (Eds.), *Concepts and Controversies in Tidal Marsh Ecology* (pp. 391-423): Springer Netherlands.

Cho, M., & Skidmore, A. (2006). A new technique for extracting the red edge position from hyperspectral data: The linear extrapolation method. *Remote sensing of environment, 101*(2), 181-193.

Cocks, T., Jenssen, R., Stewart, A., Wilson, I., & Shields, T. (1998). *The HyMapTM airborne hyperspectral sensor: the system, calibration and performance*.

Costanzo, S. D., O'Donohue, M. J., & Dennison, W. C. (2004). Assessing the influence and distribution of shrimp pond effluent in a tidal mangrove creek in north-east Australia. *Marine Pollution Bulletin, 48*(5-6), 514-525.

Curran, P. J. (1989). Remote sensing of foliar chemistry. *Remote sensing of environment, 30*(3), 271-278.

Curran, P. J., Dungan, J. L., Macler, B. A., Plummer, S. E., & Peterson, D. L. (1992). Reflectance spectroscopy of fresh whole leaves for the estimation of chemical concentration. *Remote sensing of environment, 39*(2), 153-166.

Curran, P. J., Dungan, J. L., & Peterson, D. L. (2001). Estimating the foliar biochemical concentration of leaves with reflectance spectrometry: Testing the Kokaly and Clark methodologies. *Remote sensing of environment, 76*(3), 349-359.

Dahdouh-Guebas, F., Hettiarachchi, S., Lo Seen, D., Batelaan, O., Sooriyarachchi, S., Jayatissa, L. P., et al. (2005). Transitions in Ancient Inland Freshwater Resource Management in Sri Lanka Affect Biota and Human Populations in and around Coastal Lagoons. *Current Biology, 15*(6), 579-586.

Darvishzadeh, R., Skidmore, A., Schlerf, M., Atzberger, C., Corsi, F., & Cho, M. (2008). LAI and chlorophyll estimation for a heterogeneous grassland using

hyperspectral measurements. *ISPRS Journal of Photogrammetry and Remote Sensing, 63*(4), 409-426.
De Brabanter, K., Karsmakers, P., Ojeda, F., Alzate, C., De Brabanter, J., Pelckmans, K., et al. (2010). *LS-SVMlab toolbox user's guide version 1.7*: Technical Report 10-146, Katholieke Universiteit Leuven, 2010.
Dittmar, T., & Lara, R. J. (2001). Driving Forces Behind Nutrient and Organic Matter Dynamics in a Mangrove Tidal Creek in North Brazil. *Estuarine, Coastal and Shelf Science, 52*(2), 249-259.
Efron, B., & Gong, G. (1983). A Leisurely Look at the Bootstrap, the Jackknife, and Cross-Validation. *The American Statistician, 37*(1), 36-48.
FAO. (2007). *The world's mangroves 1980-2005, FAO Forestry Paper 153.*: Food and Agriculture Organization of the United Nations, Forest Resources Division, Rome.
Feller, I. C., McKee, K. L., Whigham, D. F., & O'Neill, J. P. (2003). Nitrogen vs. phosphorus limitation across an ecotonal gradient in a mangrove forest. *Biogeochemistry, 62*(2), 145-175.
Ferwerda, J. G., & Skidmore, A. K. (2007). Can nutrient status of four woody plant species be predicted using field spectrometry? *ISPRS Journal of Photogrammetry and Remote Sensing, 62*(6), 406-414.
Fourty, T., Baret, F., Jacquemoud, S., Schmuck, G., & Verdebout, J. (1996). Leaf optical properties with explicit description of its biochemical composition: Direct and inverse problems. *Remote sensing of environment, 56*(2), 104-117.
Giri, C., Ochieng, E., Tieszen, L. L., Zhu, Z., Singh, A., Loveland, T., et al. (2011). Status and distribution of mangrove forests of the world using earth observation satellite data. *Global Ecology and Biogeography, 20*(1), 154-159.
Giri, C., Zhu, Z., Tieszen, L. L., Singh, A., Gillette, S., & Kelmelis, J. A. (2008). Mangrove forest distributions and dynamics (1975-2005) of the tsunami-affected region of Asia. *Journal of Biogeography, 35*(3), 519-528.
Gomez, C., Lagacherie, P., & Coulouma, G. (2008). Continuum removal versus PLSR method for clay and calcium carbonate content estimation from laboratory and airborne hyperspectral measurements. *Geoderma, 148*(2), 141-148.
Green, A. A., Berman, M., Switzer, P., & Craig, M. D. (1988). A transformation for ordering multispectral data in terms of image quality with implications for noise removal. *Geoscience and Remote Sensing, IEEE Transactions on, 26*(1), 65-74.
Grossman, Y. L., Ustin, S. L., Jacquemoud, S., Sanderson, E. W., Schmuck, G., & Verdebout, J. (1996). Critique of stepwise multiple linear regression for the extraction of leaf biochemistry information from leaf reflectance data. *Remote sensing of environment, 56*(3), 182-193.
Haigang, Z., Ping, S., & Chuqun, C. (2003). Retrieval of oceanic chlorophyll concentration using support vector machines. *Geoscience and Remote Sensing, IEEE Transactions on, 41*(12), 2947-2951.

Hernández, N., Kiralj, R., Ferreira, M. M. C., & Talavera, I. (2009). Critical comparative analysis, validation and interpretation of SVM and PLS regression models in a QSAR study on HIV-1 protease inhibitors. *Chemometrics and Intelligent Laboratory Systems, 98*(1), 65-77.

Heumann, B. W. (2011). Satellite remote sensing of mangrove forests: Recent advances and future opportunities. *Progress in Physical Geography, 35*(1), 87-108.

Huang, Z., Turner, B. J., Dury, S. J., Wallis, I. R., & Foley, W. J. (2004). Estimating foliage nitrogen concentration from HYMAP data using continuum removal analysis. *Remote sensing of environment, 93*(1-2), 18-29.

Huber, S., Kneubühler, M., Psomas, A., Itten, K., & Zimmermann, N. E. (2008). Estimating foliar biochemistry from hyperspectral data in mixed forest canopy. *Forest Ecology and Management, 256*(3), 491-501.

ITT Visual Information Solutions. (2009). ENVI 4.7: ITT Visual Information Solutions, Boulder, CO.

Jacquemoud, S., Verhoef, W., Baret, F., Bacour, C., Zarco-Tejada, P. J., Asner, G. P., et al. (2009). PROSPECT + SAIL models: A review of use for vegetation characterization. *Remote sensing of environment, 113*(Supplement 1), S56-S66.

Kao, W.-Y., Tsai, H.-C., & Tsai, T.-T. (2001). Effect of NaCl and nitrogen availability on growth and photosynthesis of seedlings of a mangrove species, Kandelia candel (L.) Druce. *Journal of Plant Physiology, 158*(7), 841-846.

Kawamura, K., Betteridge, K., Sanches, I. D., Tuohy, M. P., Costall, D., & Inoue, Y. (2009). Field radiometer with canopy pasture probe as a potential tool to estimate and map pasture biomass and mineral components: A case study in the Lake Taupo catchment, New Zealand. *New Zealand Journal of Agricultural Research, 52*(4), 417 - 434.

Knox, N. M., Skidmore, A. K., Schlerf, M., de Boer, W. F., van Wieren, S. E., van der Waal, C., et al. (2010). Nitrogen prediction in grasses: effect of bandwidth and plant material state on absorption feature selection. *International Journal of Remote Sensing, 31*(3), 691 - 704.

Knox, N. M., Skidmore, A. K. p., & Prins, H. H. T. p. (2010). *Observing temporal and spatial variability of forage quality.* University of Twente Faculty of Geo-Information and Earth Observation ITC, Enschede.

Kokaly, R. F. (2001). Investigating a Physical Basis for Spectroscopic Estimates of Leaf Nitrogen Concentration. *Remote sensing of environment, 75*(2), 153-161.

Kokaly, R. F., Asner, G. P., Ollinger, S. V., Martin, M. E., & Wessman, C. A. (2009). Characterizing canopy biochemistry from imaging spectroscopy and its application to ecosystem studies. *Remote sensing of environment, 113*(Supplement 1), S78-S91.

Kokaly, R. F., & Clark, R. N. (1999). Spectroscopic Determination of Leaf Biochemistry Using Band-Depth Analysis of Absorption Features and Stepwise Multiple Linear Regression. *Remote sensing of environment, 67*(3), 267-287.

Krauss, K. W., Lovelock, C. E., McKee, K. L., López-Hoffman, L., Ewe, S. M. L., & Sousa, W. P. (2008). Environmental drivers in mangrove establishment and early development: A review. *Aquatic Botany, 89*(2), 105-127.

Kupiec, J. A., & Curran, P. J. (1995). Decoupling effects of the canopy and foliar biochemicals in AVIRIS spectra. *International Journal of Remote Sensing, 16*(9), 1731 - 1739.

Lin, Y.-M., Liu, X.-W., Zhang, H., Fan, H.-Q., & Lin, G.-H. (2010). Nutrient conservation strategies of a mangrove species Rhizophora stylosa under nutrient limitation. *Plant and Soil, 326*(1), 469-479.

Lovelock, C., Ball, M., Martin, K., & Feller, I. (2009). Nutrient enrichment increases mortality of mangroves. *PLoS ONE, 4*(5).

Lovelock, C. E., Feller, I. C., Ball, M. C., Ellis, J., & Sorrell, B. (2007). Testing the Growth Rate vs. Geochemical Hypothesis for latitudinal variation in plant nutrients. *Ecology Letters, 10*(12), 1154-1163.

Lovelock, C. E., Feller, I. C., McKee, K. L., Engelbrecht, B., & Ball, M. C. (2004). The effect of nutrient enrichment on growth, photosynthesis and hydraulic conductance of dwarf mangroves in Panamá. *Ecology, 18*, 25-33.

Majeke, B., van Aardt, J., & Cho, M. (2008). Imaging spectroscopy of foliar biochemistry in forestry environments. *Southern Forests: a Journal of Forest Science, 70*(3), 275 - 285.

Martin, J.-L. (2011). Shrimp Aquaculture: From Extensive to Intensive Rearing, the Relationship with the Environment and The Key to Sustainability. In H.-J. Ceccaldi, I. Dekeyser, M. Girault & G. Stora (Eds.), *Global Change: Mankind-Marine Environment Interactions* (pp. 25-30): Springer Netherlands.

Martin, M., & Aber, J. (1997). High spectral resolution remote sensing of forest canopy lignin, nitrogen, and ecosystem processes. *Ecological Applications, 7*(2), 431-443.

Martin, M. E., Plourde, L. C., Ollinger, S. V., Smith, M. L., & McNeil, B. E. (2008). A generalizable method for remote sensing of canopy nitrogen across a wide range of forest ecosystems. *Remote sensing of environment, 112*(9), 3511-3519.

Medina, E., Cuevas, E., & Lugo, A. (2010). Nutrient relations of dwarf <i>Rhizophora mangle</i> L. mangroves on peat in eastern Puerto Rico. *Plant Ecology, 207*(1), 13-24.

Mooney, H. (1986). Photosynthesis. In M. Crawley (Ed.), *Plant ecology* (pp. 345-373). Oxford: Blackwell Scientific Publications.

Mutanga, O., Skidmore, A. K., & Prins, H. H. T. (2004). Predicting in situ pasture quality in the Kruger National Park, South Africa, using continuum-removed absorption features. *Remote sensing of environment, 89*(3), 393-408.

Nagelkerken, I., Blaber, S. J. M., Bouillon, S., Green, P., Haywood, M., Kirton, L. G., et al. (2008). The habitat function of mangroves for terrestrial and marine fauna: A review. *Aquatic Botany, 89*(2), 155-185.

Naidoo, G. (1987). Effects of Salinity and Nitrogen on Growth and Water Relations in the Mangrove, Avicennia marina (Forsk.) Vierh. *New Phytologist, 107*(2), 317-325.

Nie, Z., Han, J., Liu, T., & Liu, X. (2008). Hot Topic: Application of Support Vector Machine Method in Prediction of Alfalfa Protein Fractions by Near Infrared Reflectance Spectroscopy. *Journal of Dairy Science, 91*(6), 2361-2369.

Osuna, E., Freund, R., & Girosit, F. (2002). *Training support vector machines: an application to face detection*.

Oxmann, J., Pham, Q., Schwendenmann, L., Stellman, J., & Lara, R. (2010). Mangrove reforestation in Vietnam: the effect of sediment physicochemical properties on nutrient cycling. *Plant and Soil, 326*(1), 225-241.

Parida, A., & Jha, B. (2010). Salt tolerance mechanisms in mangroves: a review. *Trees - Structure and Function, 24*(2), 199-217.

Porder, S., Asner, G. P., & Vitousek, P. M. (2005). Ground-based and remotely sensed nutrient availability across a tropical landscape. *Proceedings of the National Academy of Sciences of the United States of America, 102*(31), 10909-10912.

Powell, N., & Osbeck, M. (2010). Approaches for understanding and embedding stakeholder realities in mangrove rehabilitation processes in Southeast Asia: lessons learnt from Mahakam Delta, East Kalimantan. *Sustainable Development*.

Reef, R., Feller, I., & Lovelock, C. (2010). Nutrition of mangroves. *Tree Physiology*.

Rönnbäck, P. (1999). The ecological basis for economic value of seafood production supported by mangrove ecosystems. *Ecological Economics, 29*(2), 235-252.

Savitzky, A., & Golay, M. J. E. (1964). Smoothing and Differentiation of Data by Simplified Least Squares Procedures. *Analytical Chemistry, 36*(8), 1627-1639.

Schachtman, D., Reid, R., & Ayling, S. (1998). Phosphorus uptake by plants: from soil to cell. *Plant Physiology, 116*(2), 447.

Schlerf, M., & Atzberger, C. (2006). Inversion of a forest reflectance model to estimate structural canopy variables from hyperspectral remote sensing data. *Remote sensing of environment, 100*(3), 281-294.

Schlerf, M., Atzberger, C., Hill, J., Buddenbaum, H., Werner, W., & Schüler, G. (2010). Retrieval of chlorophyll and nitrogen in Norway spruce (Picea abies L. Karst.) using imaging spectroscopy. *International Journal of Applied Earth Observation and Geoinformation, 12*(1), 17-26.

Scholkopf, B., Kah-Kay, S., Burges, C. J. C., Girosi, F., Niyogi, P., Poggio, T., et al. (1997). Comparing support vector machines with Gaussian kernels to radial basis function classifiers. *Signal Processing, IEEE Transactions on, 45*(11), 2758-2765.

Schölkopf, B., Smola, A. J., Williamson, R. C., & Bartlett, P. L. (2000). New Support Vector Algorithms. *Neural Computation, 12*(5), 1207-1245.

Serrano, L., Peñuelas, J., & Ustin, S. L. (2002). Remote sensing of nitrogen and lignin in Mediterranean vegetation from AVIRIS data: Decomposing

biochemical from structural signals. *Remote sensing of environment, 81*(2-3), 355-364.

Shah, A. R., Agarwal, K., Baker, E. S., Singhal, M., Mayampurath, A. M., Ibrahim, Y. M., et al. (2010). Machine learning based prediction for peptide drift times in ion mobility spectrometry. *Bioinformatics, 26*(13), 1601-1607.

Shmilovici, A. (2005). Support Vector Machines. In O. Maimon & L. Rokach (Eds.), *Data Mining and Knowledge Discovery Handbook* (pp. 257-276): Springer US.

Sidik, A. (2009). *The changes of mangrove ecosystem in Mahakam delta, Indonesia*. Paper presented at the The South China Sea Conference 2008. The South China Sea: Sustaining Ocean Productivities, Maritime Communities and the Climate.

Smith, M.-L., Ollinger, S. V., Martin, M. E., Aber, J. D., Hallett, R. A., & Goodale, C. L. (2002). Direct Estimation of Aboveground Forest Productivity through Hyperspectral Remote Sensing of Canopy Nitrogen. *Ecological Applications, 12*(5), 1286-1302.

Smith, M. L., Martin, M. E., Plourde, L., & Ollinger, S. V. (2003). Analysis of hyperspectral data for estimation of temperate forest canopy nitrogen concentration: comparison between an airborne (AVIRIS) and a spaceborne (Hyperion) sensor. *Geoscience and Remote Sensing, IEEE Transactions on, 41*(6), 1332-1337.

Smola, A., & Schölkopf, B. (2004). A tutorial on support vector regression. *Statistics and Computing, 14*(3), 199-222.

Sulong, I., Mohd-Lokman, H., Mohd-Tarmizi, K., & Ismail, A. (2002). Mangrove Mapping Using Landsat Imagery and Aerial Photographs: Kemaman District, Terengganu, Malaysia. *Environment, Development and Sustainability, 4*(2), 135-152.

Suykens, J., Van Gestel, T., & De Brabanter, J. (2002). *Least squares support vector machines*: World Scientific Pub Co Inc.

Tam, N. F. Y., Wong, A. H. Y., Wong, M. H., & Wong, Y. S. (2009). Mass balance of nitrogen in constructed mangrove wetlands receiving ammonium-rich wastewater: Effects of tidal regime and carbon supply. *Ecological Engineering, 35*(4), 453-462.

The MathWorks. (2010). Matlab R2010a: The MathWorks, Natick, MA.

Thissen, U., Pepers, M., Üstün, B., Melssen, W. J., & Buydens, L. M. C. (2004). Comparing support vector machines to PLS for spectral regression applications. *Chemometrics and Intelligent Laboratory Systems, 73*(2), 169-179.

Thissen, U., Üstün, B., Melssen, W. J., & Buydens, L. M. C. (2004). Multivariate Calibration with Least-Squares Support Vector Machines. *Analytical Chemistry, 76*(11), 3099-3105.

Tsai, F., & Philpot, W. (1998). Derivative Analysis of Hyperspectral Data. *Remote sensing of environment, 66*(1), 41-51.

Üstün, B., Melssen, W. J., & Buydens, L. M. C. (2007). Visualisation and interpretation of Support Vector Regression models. *Analytica Chimica Acta, 595*(1-2), 299-309.

Ukpong, I. (2000). Ecological classification of Nigerian mangroves using soil nutrient gradient analysis. *Wetlands Ecology and Management, 8*(4), 263-272.

Vapnik, V. (1995). The nature of statistical learning: springer New York, NY.

Verhoef, W., & Bach, H. (2007). Coupled soil-leaf-canopy and atmosphere radiative transfer modeling to simulate hyperspectral multi-angular surface reflectance and TOA radiance data. *Remote sensing of environment, 109*(2), 166-182.

Walters, B. B., Rönnbäck, P., Kovacs, J. M., Crona, B., Hussain, S. A., Badola, R., et al. (2008). Ethnobiology, socio-economics and management of mangrove forests: A review. *Aquatic Botany, 89*(2), 220-236.

Walton, M. E. M., Samonte-Tan, G. P. B., Primavera, J. H., Edwards-Jones, G., & Le Vay, L. (2006). Are mangroves worth replanting? The direct economic benefits of a community-based reforestation project. *Environmental Conservation, 33*(04), 335-343.

Wang, F.-m., Huang, J.-f., & Lou, Z.-h. (2010). A comparison of three methods for estimating leaf area index of paddy rice from optimal hyperspectral bands. *Precision Agriculture*, 1-9.

Wessman, C. A., Aber, J. D., Peterson, D. L., & Melillo, J. M. (1988). Remote sensing of canopy chemistry and nitrogen cycling in temperate forest ecosystems. *Nature, 335*(6186), 154-156.

Wold, S., Sjöström, M., & Eriksson, L. (2001). PLS-regression: a basic tool of chemometrics. *Chemometrics and Intelligent Laboratory Systems, 58*(2), 109-130.

Wright, I. J., Reich, P. B., Westoby, M., Ackerly, D. D., Baruch, Z., Bongers, F., et al. (2004). The worldwide leaf economics spectrum. *Nature, 428*(6985), 821-827.

Yates, E., Ashwath, N., & Midmore, D. (2002). Responses to nitrogen, phosphorus, potassium and sodium chloride by three mangrove species in pot culture. *Trees - Structure and Function, 16*(2), 120-125.

Zhang, J.-E., Liu, J.-L., Ouyang, Y., Liao, B.-W., & Zhao, B.-L. (2010). Removal of nutrients and heavy metals from wastewater with mangrove Sonneratia apetala Buch-Ham. *Ecological Engineering, 36*(6), 807-812.

Zhou, H.-C., Wei, S.-D., Zeng, Q., Zhang, L.-H., Tam, N. F.-y., & Lin, Y.-M. (2010). Nutrient and caloric dynamics in Avicennia marina leaves at different developmental and decay stages in Zhangjiang River Estuary, China. *Estuarine, Coastal and Shelf Science, 87*(1), 21-26.

6. Appendix 1: Maps of collected samples

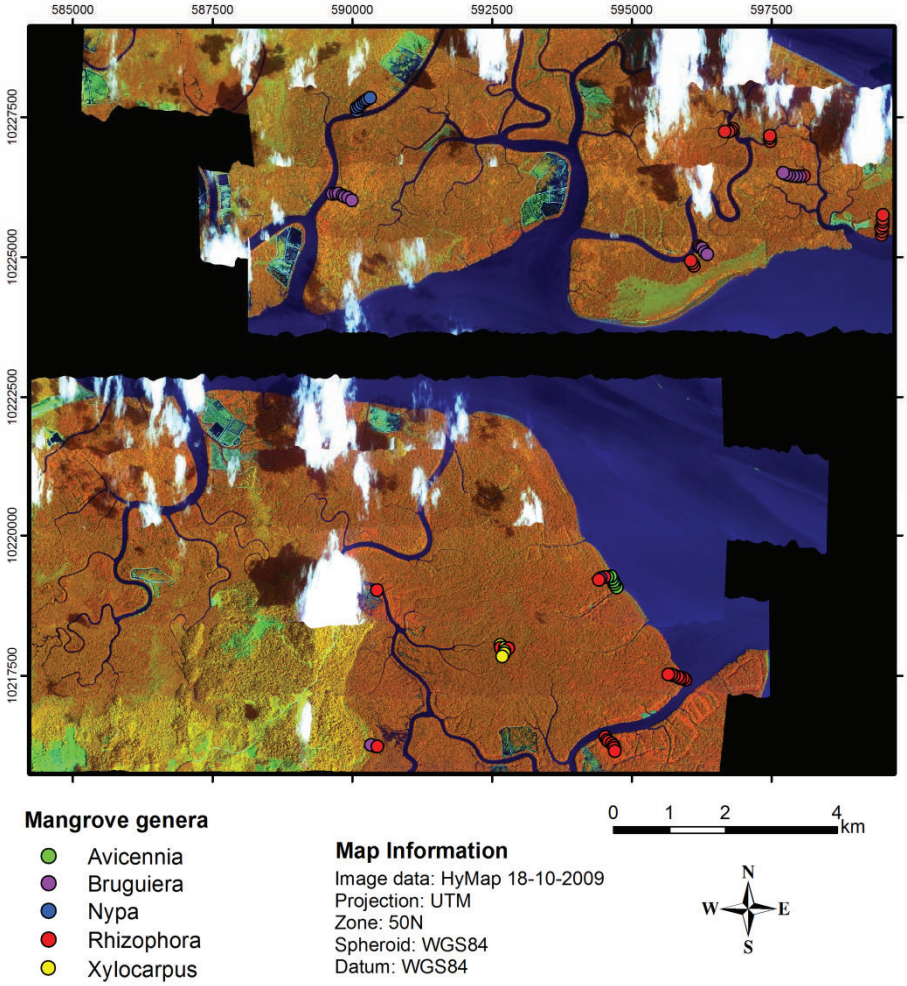

Figure 17: Map of Berau study area showing collected samples.

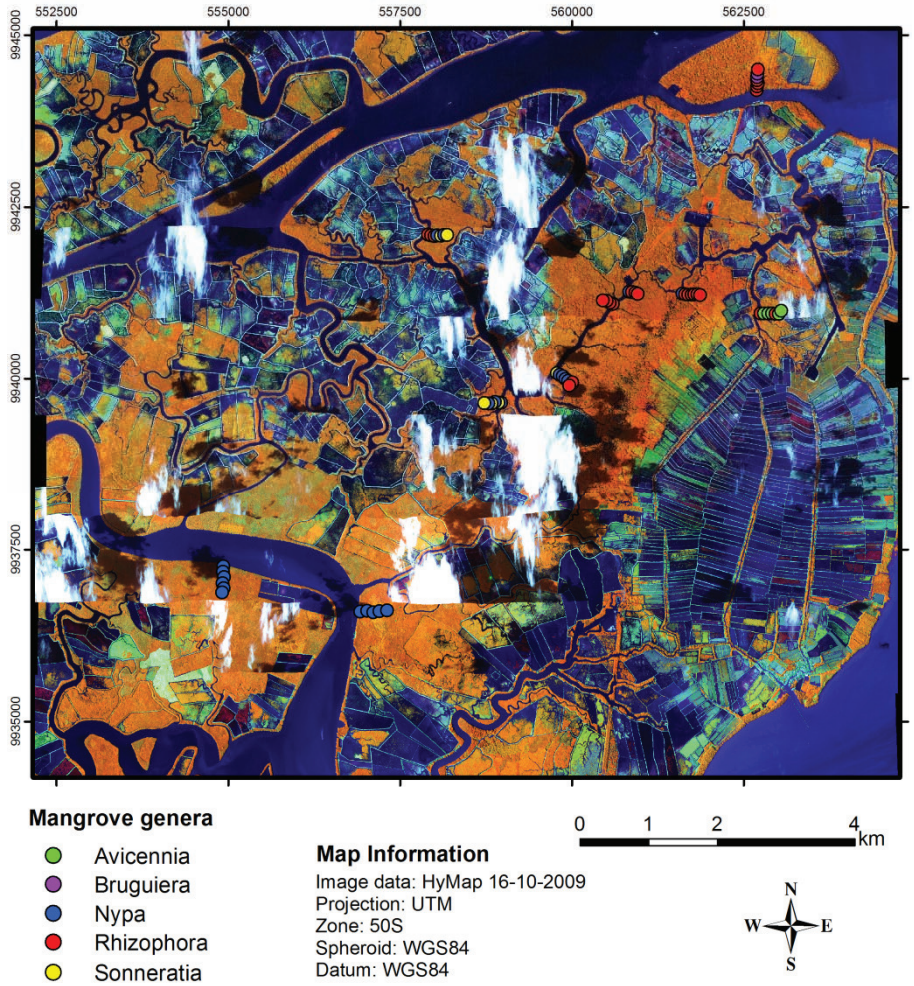

Figure 18: Map of Mahakam study area showing collected samples.